Chapter 2

CALCULATION AND VERIFICATION OF SOURCE TERMS

Paul P. Whalen
Los Alamos National Laboratory

The number of particles or quanta of radiation emerging from a bomb, and their distributions in energy and direction, are called its "source terms" or its "leakage spectra". They depend on the number of fissions that took place (see Chapter 1) and on the nature and position of the materials in the bomb. The source terms for the neutrons and gamma rays emitted by the fission products produced by the bombs are discussed in Chapter 3 and in Appendixes 3-4 and 3-5. The source terms form the starting point of the calculations of the doses received by the people in Hiroshima and Nagasaki as reported in later chapters.

The source terms were calculated with computer programs that followed the penetration of the radiations emitted in fission, and their secondary radiations, through the material of the bomb and into a mass of air surrounding the bomb. Hydrodynamic effects from the air had to be included in the calculation.

The source terms are the spectra at the surface of the exploding bombs. They are treated, however, as the spectra from point sources to simplify subsequent calculations. The simplification is justified because the differences between the fluences calculated for a source of nonzero size and a point source do not differ appreciably at the closest point of interest, the ground at the hypocenter.

The source terms contain all the radiations emitted while the bomb materials are fissioning. The fissions are completed in a few microseconds. The rates of emission during this interval were not calculated; the source terms are the numbers for the whole interval.

SOURCE TERMS FOR THE HIROSHIMA AND NAGASAKI BOMBS

The calculation of the source terms was described earlier.[1,2] Those descriptions are summarized here.

Calculations

Monte Carlo techniques were used to calculate the source spectra. Special purpose

versions of the MCNP code[3] that calculate the transport of neutrons and gamma rays in hot, moving material were used in conjunction with explosion codes that calculate the temperature and the hydrodynamic motion of the parts of the bomb resulting from the nuclear energy released within them. Although there was relative motion in the interior of the exploding bomb, the fissions were essentially over before the case of the bomb could break apart because a nonnuclear deformation wave, traveling at the speed of sound, did not have time to reach the casing. Therefore, there was some rearrangement of the material the radiation had to pass through to emerge from the bomb, but there was no major reduction in that material due to cracks in the casing.

The MCNP codes can use a number of different cross-section libraries. Most of the source spectrum calculations used ENDF/B[4] cross sections in a continuous energy format. The Hiroshima and Nagasaki bomb calculations done in 1975 by Preeg[5] used ENDF/B III cross sections. The present Hiroshima calculations used ENDF/B V cross sections, in general, with some new Los Alamos cross-section evaluations that will be in the upcoming ENDF/B VI library. Calculated neutron spectra were not sensitive to these different versions of the ENDF/B libraries, but the calculated gamma-ray spectra changed greatly (see below) with the use of ENDF/B Version III or Version V cross sections.

In addition to the continuous energy libraries, the MCNP code can use cross-section libraries in discrete energy (multigroup) format. The difference between these formats is shown in Figure 1 where the total cross section for iron is plotted from the continuous energy library and from a 225 group library generated from the same ENDF/B V data. The figure is in two parts; Figure 1a covers a broad energy range to show the extent of the resonance structure; Figure 1b covers only the range from 0.2 to 0.3 MeV to emphasize the difference between the continuous and the multigroup representations. Calculated neutron spectra for the Hiroshima explosion and the Hiroshima bomb replica (see below) are sensitive to this change in format as shown below.

In the Monte Carlo source calculations, neutron and gamma-ray "particles" and their progeny are tracked from emission to absorption or escape from the system. At escape, information about the vector velocity of the particle is available in a three-dimensional coordinate system. The "weights" of neutrons and gamma rays emerging from the Hiroshima explosion calculations were tallied both by energy and by particle direction relative to the axis of the bomb. The directions were tallied into twenty equal, polar, solid-angle bins. Only energy tallies were made from calculations for the Nagasaki explosion.

Neutron Source Terms

Table 1 gives the number of neutrons per kiloton (kt) in each energy bin (i.e., summed over the polar-angle bins) calculated for Hiroshima and Nagasaki.[2] The number of neutrons in each of the polar-angle bins is given in Whalen.[2]

For Figure 2, the number of neutrons per kt, ΔN, in each bin was divided by the difference, $\Delta(\ln(E))$, in the logarithms of the energies on the upper and lower sides of the bin. The quotient, $\Delta N/\Delta(\ln(E))$, is a histogram that approximates the distribution, $dN/d(\ln(E))$, of the number of neutrons per kt in the logarithm of the energy. Since the differential of the logarithm, $d(\ln(E))$, equals dE/E, the ordinate on the figure is labeled E (dN/dE). The reason for employing this method of plotting is because, when E (dN/dE) is plotted versus ln(E) (as

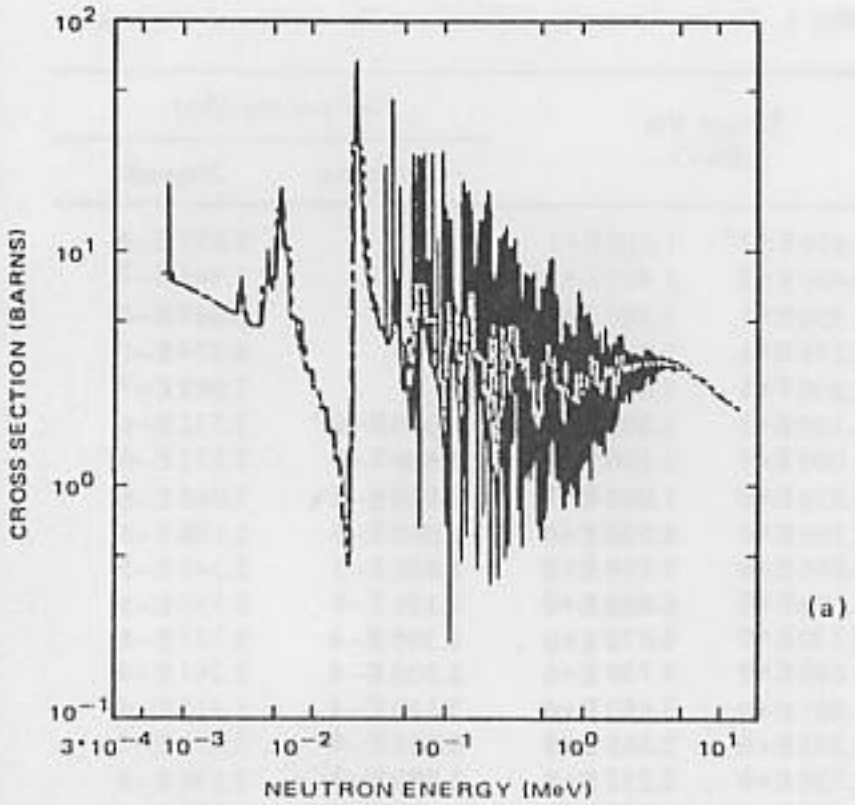

Figure 1. Total neutron cross section for iron. (a) The dotted line is from a continuous-energy library; the solid line is a histogram from a 225-group library. Both curves were generated from the same ENDF/B V data. (b) The curves of (a) for the narrow energy range 0.2 to 0.3 MeV to show more clearly the difference in the two cross section libraries.

Table 1. Source Terms for Neutrons at Hiroshima and Nagasaki.

Energy Bin (MeV)		Neutron (mol/kt)	
		Hiroshima	Nagasaki
1.450 E+1[a]	1.600 E+1		9.657 E−8
1.400 E+1	1.450 E+1		1.441 E−7
1.350 E+1	1.400 E+1		3.648 E−8
1.275 E+1	1.350 E+1		4.974 E−7
1.200 E+1	1.275 E+1		7.669 E−7
1.100 E+1	1.200 E+1	4.040 E−6[b]	1.531 E−6
1.000 E+1	1.100 E+1	3.600 E−6	2.173 E−6
8.830 E+0	1.000 E+1	7.010 E−6	7.068 E−6
7.790 E+0	8.830 E+0	2.050 E−5	1.188 E−5
6.880 E+0	7.790 E+0	1.880 E−5	2.249 E−5
6.070 E+0	6.880 E+0	4.120 E−5	3.596 E−5
4.730 E+0	6.070 E+0	1.300 E−4	9.721 E−5
3.680 E+0	4.730 E+0	2.200 E−4	1.261 E−4
2.865 E+0	3.680 E+0	3.510 E−4	1.415 E−4
2.232 E+0	2.865 E+0	6.850 E−4	3.021 E−4
1.738 E+0	2.232 E+0	1.080 E−3	2.198 E−4
1.353 E+0	1.738 E+0	1.690 E−3	1.844 E−4
1.060 E+0	1.353 E+0	3.160 E−3	1.495 E−4
8.230 E−1	1.060 E+0	5.150 E−3	1.161 E−4
6.400 E−1	8.230 E−1	6.080 E−3	1.231 E−4
5.000 E−1	6.400 E−1	1.210 E−2	1.347 E−4
3.030 E−1	5.000 E−1	2.850 E−2	1.232 E−4
1.840 E−1	3.030 E−1	2.510 E−2	1.055 E−4
6.760 E−2	1.840 E−1	4.350 E−2	1.672 E−4
2.480 E−2	6.760 E−2	1.620 E−2	9.102 E−5
9.120 E−3	2.480 E−2	2.750 E−2	6.911 E−5
3.350 E−3	9.120 E−3	2.390 E−3	8.214 E−5
1.235 E−3	3.350 E−3	1.830 E−3	6.432 E−4
4.540 E−4	1.235 E−3	1.110 E−3	4.369 E−2
1.670 E−4	4.540 E−4	3.610 E−4	1.179 E−1
6.140 E−5	1.670 E−4	9.020 E−5	6.950 E−2
2.260 E−5	6.140 E−5	2.310 E−5	2.792 E−2
8.320 E−6	2.260 E−5		8.677 E−3
3.060 E−6	8.320 E−6		2.202 E−3
1.130 E−6	3.060 E−6		4.413 E−4
4.140 E−7	1.130 E−6		9.638 E−5
1.520 E−7	4.140 E−7		2.072 E−5
1.390 E−10	1.520 E−7		4.552 E−6
Total (mol/kt)		1.773 E−1	2.734 E−1

[a]Read as 1.45×10^{1} to 1.600×10^{1} MeV, or 14.5 to 16.0 MeV.
[b]Neutrons between 11 and 20 MeV.

it is in Figure 2 and other figures; the numbers given on the abscissa are placed at the values of their logarithm), then equal areas anywhere under the curve represent equal numbers of neutrons. Also, the total area under a curve represents the total number of neutrons per kt. The total number emitted at Hiroshima was 0.177 moles per kt or 1.07×10^{23} neutrons per

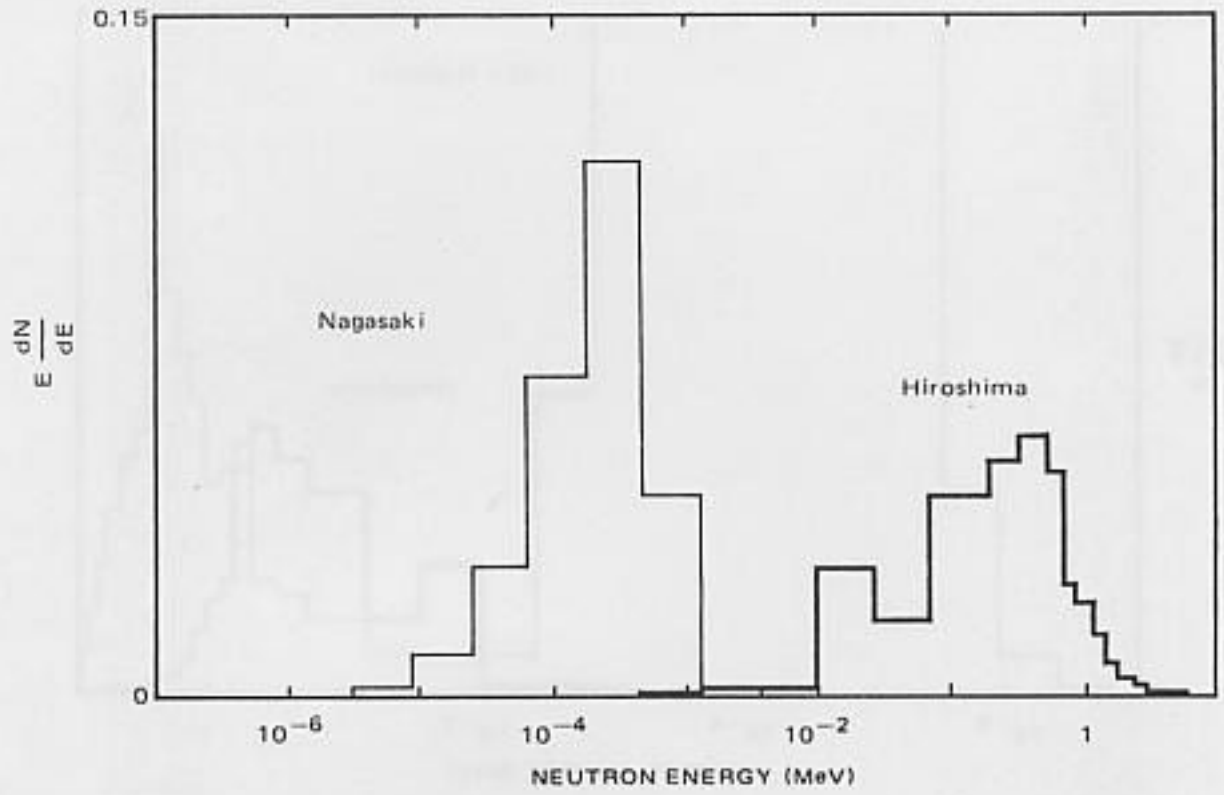

Figure 2. Distribution in the logarithm of the energy of neutrons emitted from the Hiroshima and Nagasaki bombs.

kt and at Nagasaki was 0.273 moles per kt or 1.65×10^{23} neutrons per kt.

The figure shows that the spectra for the two cities differ markedly. The Nagasaki spectrum has a large peak near a few tenths of a kilovolt. This low-energy peak is a result of neutrons interacting with the high explosive debris around the bomb, losing much of their energy, and coming into thermal equilibrium with the high temperature debris. The Hiroshima spectrum has no such peak because the neutrons did not encounter nearly so much efficient slowing down material.

Figure 2 does not convey, however, the correct impression regarding what dose the people received from the neutrons. Most of the neutron dose, even at Nagasaki, was due to the high-energy neutrons, about 1 MeV and higher, emitted from the bomb. Most of the low-energy neutrons were absorbed in the intervening atmosphere. In Figure 2 these high-energy neutrons for Nagasaki are not even visible; therefore, in Figure 3, the curves are redrawn with the ordinates for Nagasaki multiplied by 100. Now the shape of the spectrum for the Nagasaki high-energy neutrons can be seen. Because there are so few neutrons per kt under this high-energy part of the curve for Nagasaki compared with the number for Hiroshima (and because the relative total number of neutrons is only slightly changed by the difference in the yields at the two cities), the neutron doses at Nagasaki are smaller than those at Hiroshima.

The neutrons emerging from the bombs were affected by the material they had to penetrate, but in different ways at Hiroshima and Nagasaki. The neutrons at Hiroshima were strongly inelastically scattered in the heavy metal of the bomb. The result can be seen in Figure 3. At the high energies, the Nagasaki spectrum has roughly the shape of an unat-

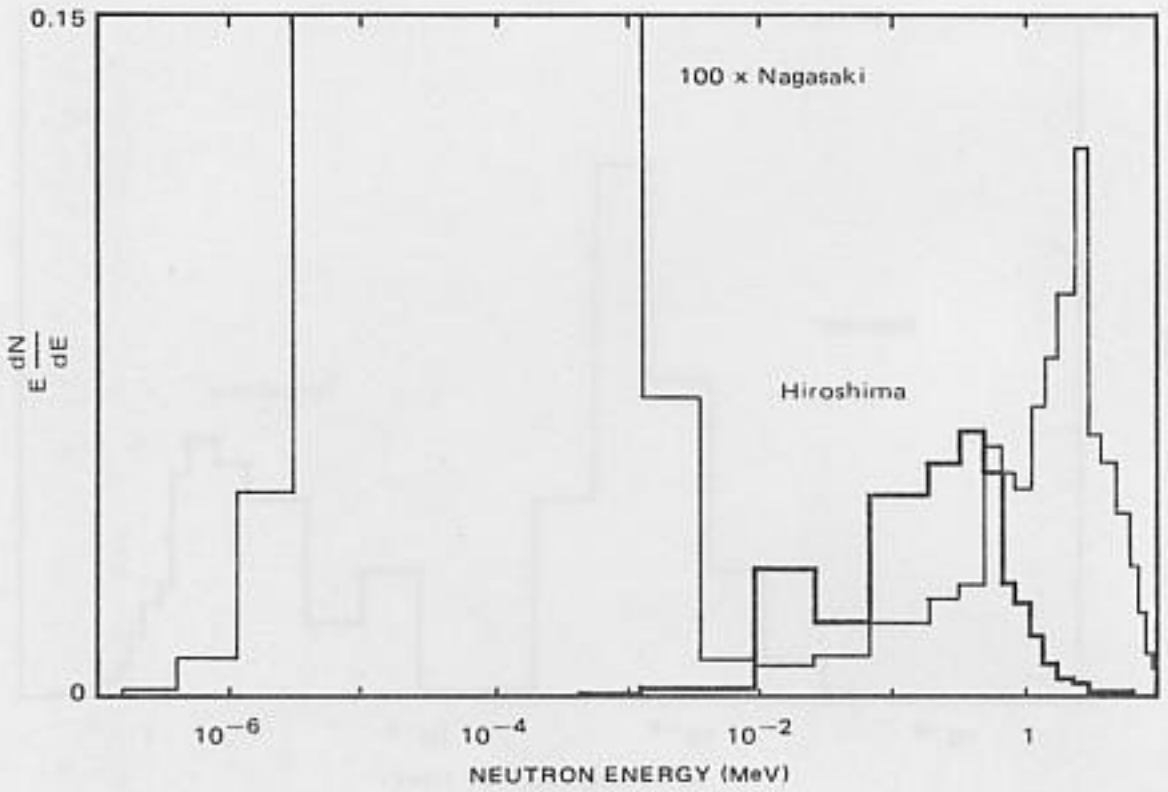

Figure 3. Distribution in the logarithm of the energy of neutrons emitted from the Hiroshima and Nagasaki bombs. The ordinates of the distribution for Nagasaki are multiplied by 100 to make the high-energy part of the spectrum visible.

tenuated fission source; the Hiroshima spectrum shows comparatively fewer neutrons with increasing energy.

Gamma-Ray Source Terms

Table 2 gives the gamma-ray source terms; Figure 4 shows the distributions in the logarithm of the energy of the number of gamma rays per kt. The calculations for the gamma rays require fewer energy groups than those for neutrons because their cross sections change more slowly with energy. While the distributions for the two cities differ somewhat in shape, the difference does not present as much of a problem to the dosimetry as the difference in shape for neutrons. In part, the shape is unimportant because, as will be seen in Chapter 3, these prompt primary gamma rays make only a relatively small contribution to the doses to the people.

The figure shows that many more gamma rays per kt were emitted from the Nagasaki bomb than from the Hiroshima bomb. The difference, both in number and in spectral shape, resulted from the difference in construction of the two bombs.

Calculations of source terms began in the 1960s. The first results made available to a wider audience were due to Preeg.[5] His neutron source terms were in good agreement with those in Table 1; his gamma-ray source terms, however, were quite different. The difference was due to a large change in the gamma-ray interaction coefficients given in the ENDF/B files in the time between the two sets of calculations. Figures 5 and 6 compare his gamma-ray spectra with those from the present work.

Table 2. Source Terms for Gamma Rays at Hiroshima and Nagasaki.

Energy Bin (MeV)		Gamma rays (mol/kt)	
		Hiroshima	Nagasaki
9	10	2.600E−5	9.939E−7
8	9	3.380E−5	7.935E−6
7	8	1.220E−4	5.828E−5
6	7	5.520E−5	2.992E−5
5	6	6.130E−5	7.413E−5
4	5	1.050E−4	3.606E−4
3	4	1.930E−4	4.983E−3
2.5	3	1.710E−4	3.245E−5
2	2.5	2.400E−4	6.489E−3
1.5	2	2.700E−4	8.615E−3
1	1.5	4.540E−4	9.351E−3
0.8	1	8.040E−4	4.440E−3
0.6	0.8	4.930E−4	5.524E−3
0.5	0.6	3.410E−4	3.656E−3
0.4	0.5	3.430E−4	3.884E−3
0.3	0.4	3.740E−4	3.724E−3
0.2	0.3	5.050E−4	3.679E−3
0.1	0.2	4.190E−4	3.863E−3
0.05	0.1	3.110E−5	9.494E−4
0	0.05	1.860E−6	2.723E−5
Total (mol/kt)		5.043E−3	6.296E−2

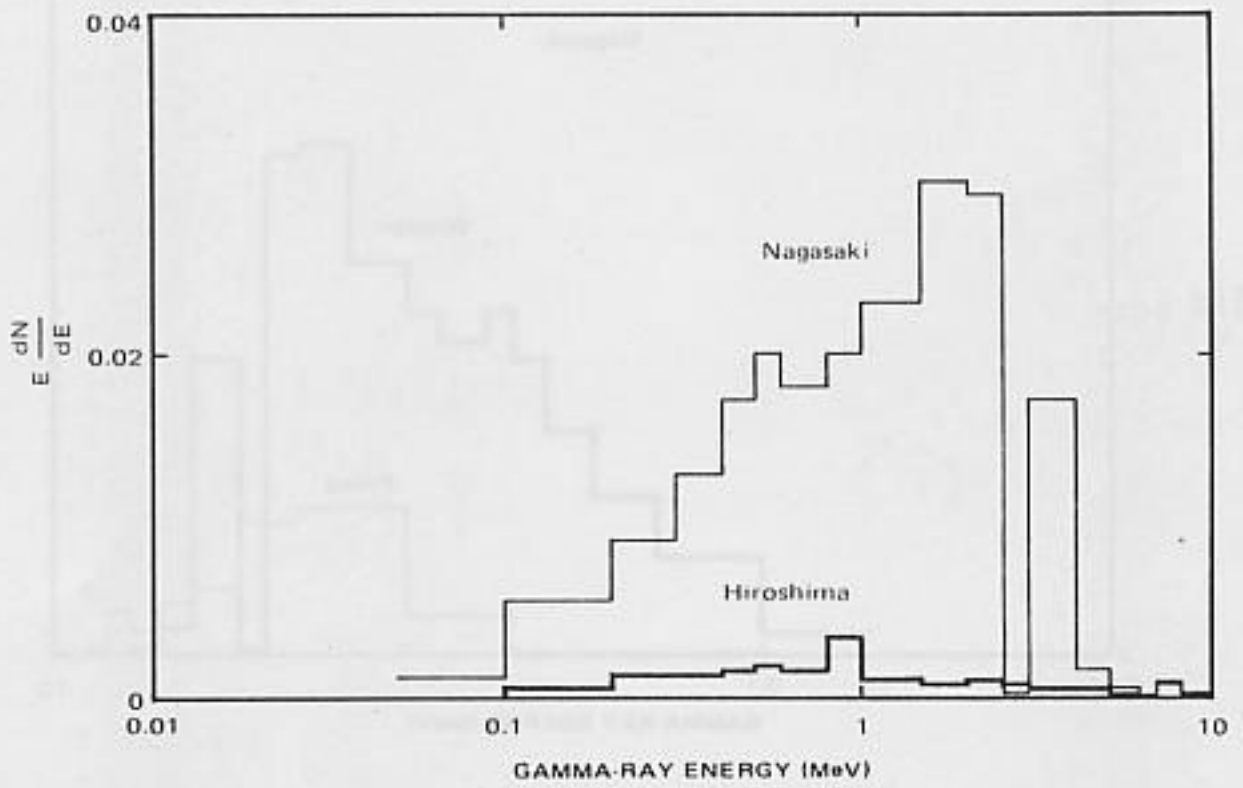

Figure 4. Distribution in the logarithm of the energy of gamma rays emitted from the Hiroshima and Nagasaki bombs.

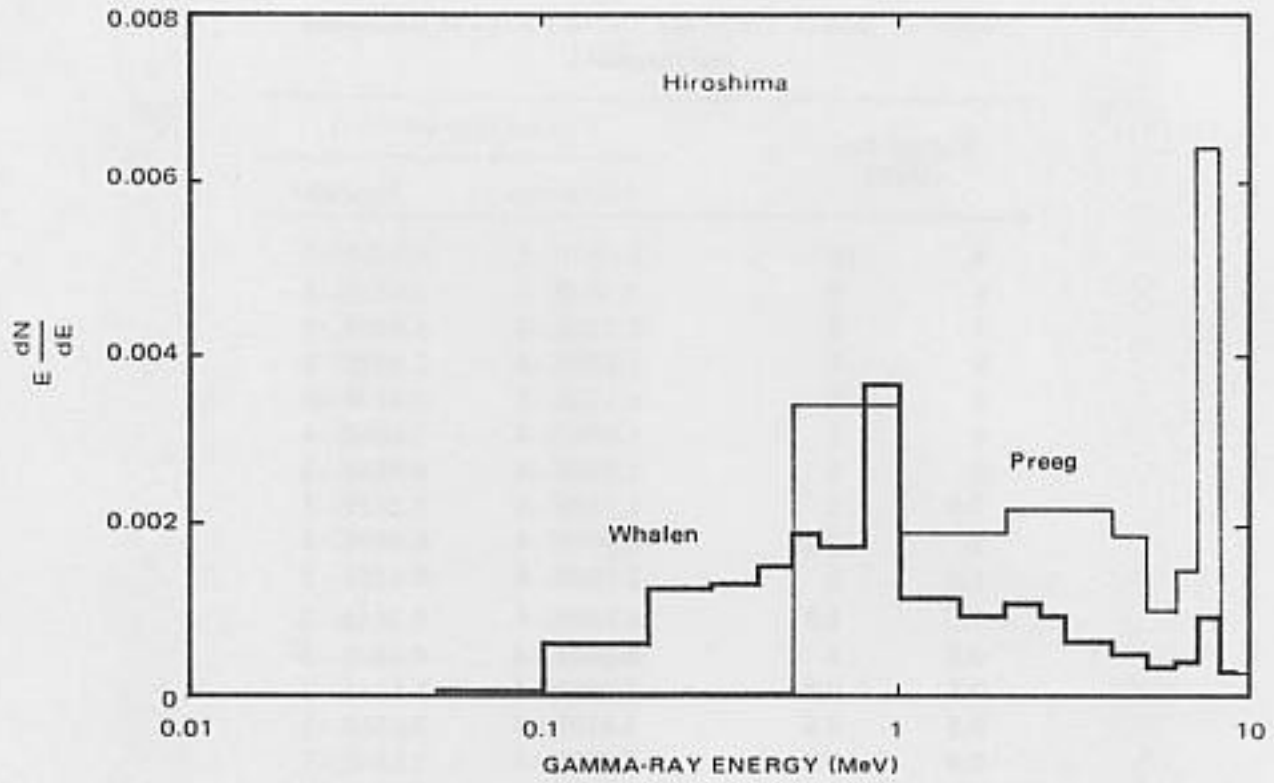

Figure 5. Change for Hiroshima in the gamma-ray distrution in the logarithm of the energy brought about by changes in ENDF/B.

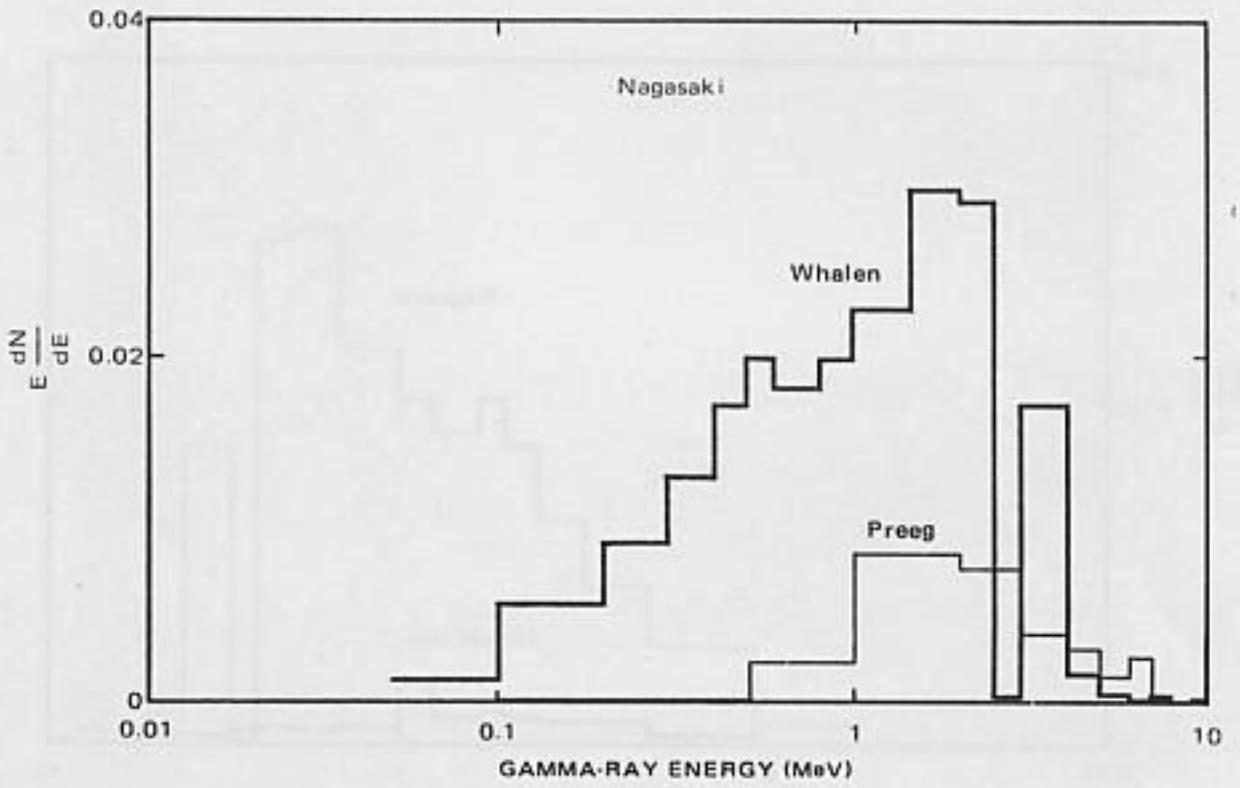

Figure 6. Change for Nagasaki in the gamma-ray distribution in the logarithm of the energy brought about by changes in ENDF/B.

SOURCE TERM VERIFICATION

Comparison of several different kinds of measurements with calculations made using the same computer codes used to calculate the source terms for the Hiroshima and Nagasaki bombs provides a basis for judging the validity of the codes and the cross sections used for the source terms.

Project ICHIBAN

As part of the ICHIBAN (T65D) project,[6] Thorngate et al[7] measured the leakage spectrum at a bare metal reactor (also called ICHIBAN). This spherical reactor was intended to model the waist configuration of the Hiroshima bomb. The leakage spectrum was calculated as an initial step in the present reassessment program.[2] The calculations seriously disagreed with the Thorngate measurements. The calculation was in much better agreement with a previously unreported measurement by Biggers of the ICHIBAN leakage spectrum. Measurements of the leakage spectrum at the waist of the Hiroshima bomb replica (below) also disagreed with the Thorngate measurements while supporting the leakage spectrum as measured by Biggers and as calculated.[2] The reason for the disagreement of the measurements by Thorngate et al[7] with other measurements and with calculations is not known.

Use of Leakage Spectra in Transport Calculations

The same computer programs used to obtain the source terms for the Hiroshima and Nagasaki bombs were used to compute the leakage spectra for an unshielded reactor on a large tower (BREN - one of the ICHIBAN experiments), a similar reactor used by the Army Pulse Radiation Division (APRD), and several bombs exploded in weapons tests in Nevada. These leakage spectra were used as the input for transport calculations. The results of the transport calculations compared satisfactorily with measurements of different types (see Chapter 3 and Appendixes 3-2, 3-3, 3-4, and 5-1). The comparison, of course, was with the combined leakage spectra and air transport calculations and was thus less direct than comparisons with measured leakage spectra.

The Hiroshima Bomb (Little Boy) Replica

The bomb exploded over Hiroshima was a gun assembly in which one subcritical mass of uranium was fired down a gun barrel toward another subcritical mass of uranium. The explosion occured when the two subcritical masses of uranium together constituted a supercritical mass in the environment of the gun. A gun assembly, however, can be operated as a low power reactor (critical assembly) by reducing the total mass of uranium to an amount just sufficient to be at delayed critical rather than supercritical in the environment of the gun. Such a critical assembly was constructed at the Los Alamos Critical Assembly Facility in 1982 from nonfissile components of a duplicate of the Hiroshima bomb that had been stored at Los Alamos and from an appropriate mass of uranium.[8] This assembly has been referred to as the "Little Boy Replica" (reactor) after the wartime code name for the Hiroshima weapon. It was intended that measurements on this reactor would provide benchmark data for testing the transport codes and cross sections used in the Hiroshima explosion calculation.

The nonfissile components of the replica were mounted, with the bomb nose up, on the

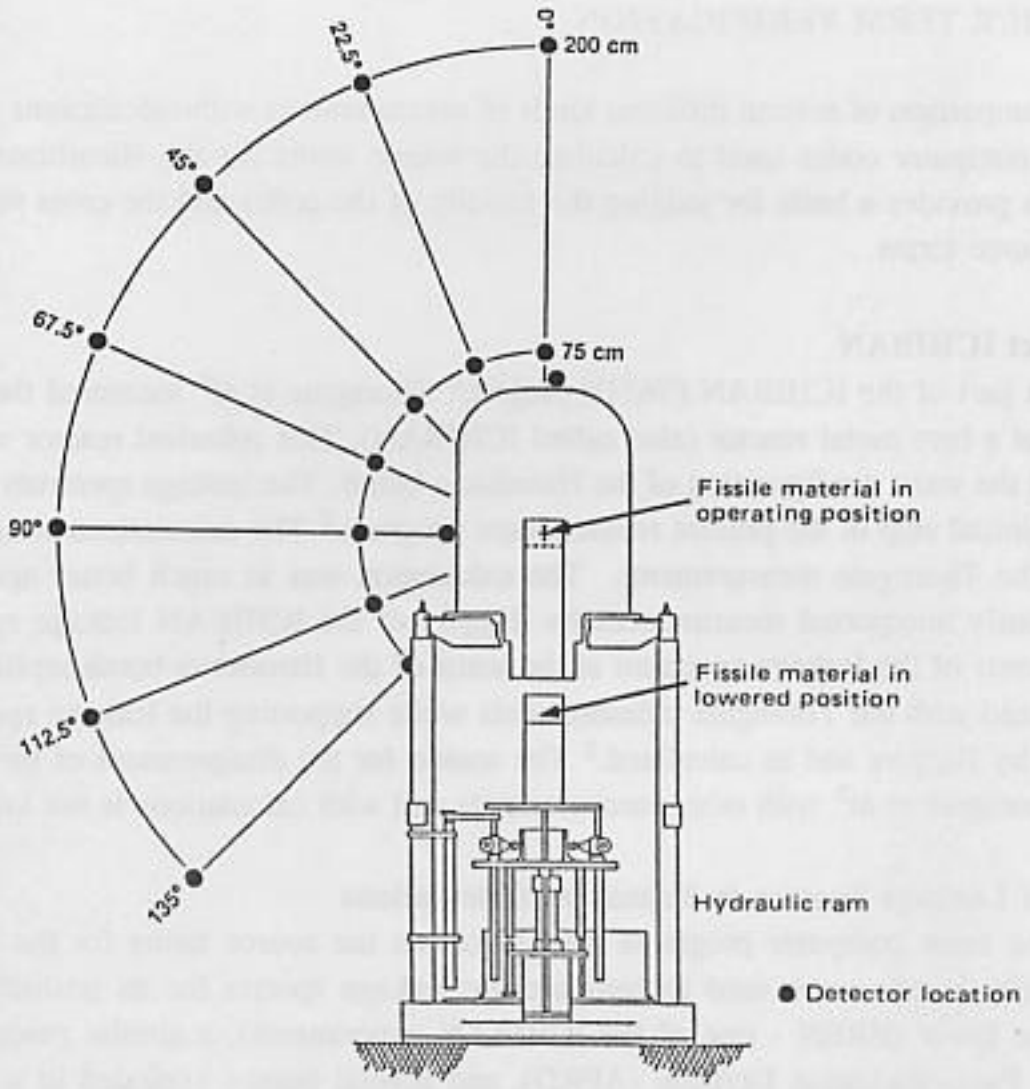

Figure 7. The Hiroshima bomb (Little Boy) replica and the positions at which measurements were made.

platform of the Comet Critical Assembly Machine. A uranium core could be raised into the interior of the assembly by a hydraulic ram and screw mechanism of the machine. The only changes made in the working parts of the bomb were the shortening of the gun barrel and the use of a reduced mass of fissile material. Shortening the gun barrel was necessary to allow complete withdrawl of the core in the limitations of the stroke of the hydraulic ram. The configuration is illustrated in Figure 7. Also shown in the figure are the locations of points for which neutron spectra were calculated. The Comet Assembly Machine is usually located in Kiva II, one of three thick-walled concrete buildings located several hundred meters from the central control room and office buildings of the Los Alamos Critical Assembly Facility. The location of the Little Boy reactor in Kiva II is shown in Figure 8. Also shown are the locations in the kiva of two other critical assembly devices, Big Ten and Flat Top. Both of these assemblies have uranium reflectors, but neither was made active during the measurement period.

The approximately 1-foot thick concrete floor, walls, and roof of Kiva II contributed background to measurements made inside the kiva. When operated in the kiva, the center of the core was 2.31 m above floor level, 4.2 m from the nearest wall, and 5.6 m below

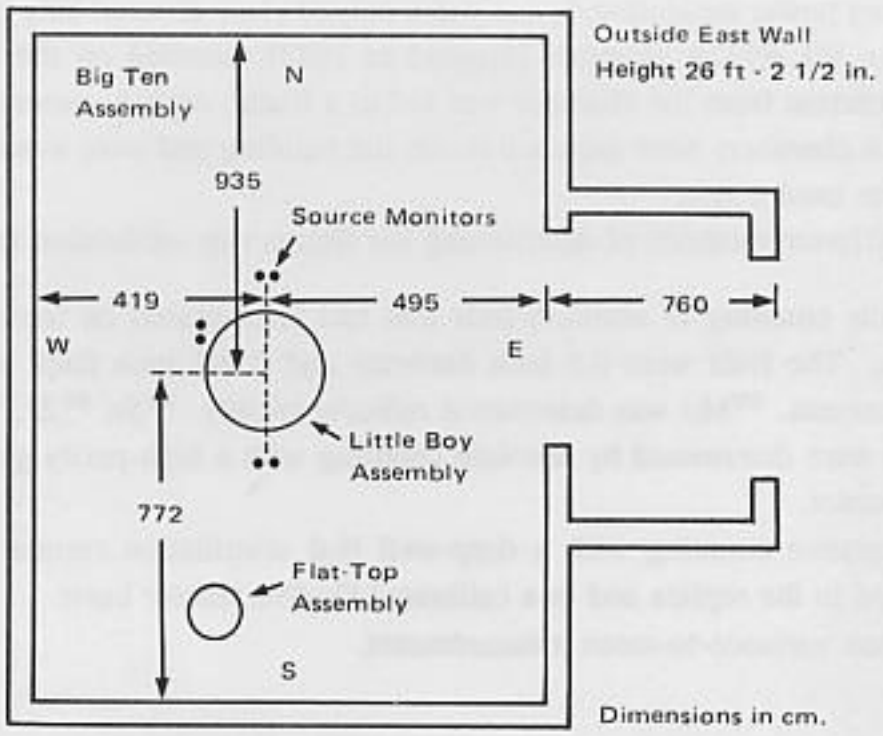

Figure 8. Floor plan of the building (kiva) in which the Little Boy reactor was used when not outdoors.

roof level. To reduce background for the experimenters, the entire assembly was moved out of the kiva and operated in an open area approximately 20 m from the kiva. The Comet Assembly Machine, when outside, was mounted on a stand that raised the core center to 4 m above the ground.

Criticality Measurements. Two kinds of measurements were made for the reassessment program. For one, the full amount of fissionable material used in the bomb was placed in the replica and the two fissionable parts brought closer and closer together to determine the separation at which the assembly first became delayed critical. This situation duplicated the conditions in the bomb itself. The calculation of the separation, however, depends only on the properties of the assembly; it does not depend on the thermal and hydrodynamic responses of the exploding bomb. The calculated delayed-critical separation was 0.008 cm less than the measured distance and was within the ± 0.010 cm error bar of the measurement. The calculation was made using continuous-energy ENDF/B cross sections with no adjustments.

Similar calculations of the Hiroshima bomb explosion made with the same cross sections imply that the maximum yield of the Hiroshima bomb explosion was 15 ± 2 kt. The actual yield, of course, could be any value less than the maximum. The critical separation measurement rules out the possibility of yields greater than 17 kt. The rest of the studies with the replica were made in the reactor mode (with the reduced amount of uranium).

Calibration of the Replica. In making measurements at the Little Boy Replica, experimenters[9] were given the power level at the time of their measurement. They converted this level into the fission rate within the reactor with a calibration factor.

The primary power measuring device was a polyethylene covered BF_3 ionization chamber (Westinghouse WL-6937A chamber installed in 1982) mounted on the stand holding the replica. The current from the chamber was fed to a linear, digital, current integrator. Other BF_3 ionization chambers were mounted inside the building and were available for use when the replica was used inside.

Several different methods of determining the fission-rate calibration factor were used:

1. Absolute counting of uranium foils that had been placed on top of the core of the replica. The foils were 0.5 inch diameter and 0.001 inch thick and were wrapped in aluminum. ^{99}Mo was determined radiochemically. ^{91}Sr, ^{96}Zr, ^{99}Mo, ^{103}Ru, and ^{140}Ba were determined by absolute counting with a high-purity germanium gamma-ray counter.
2. Comparative counting with a deep-well NaI scintillation counter of uranium foils exposed in the replica and in a calibrated Godiva reactor burst.
3. Feynman variance-to-mean measurements.

Calibration runs were made on 6 November 1982 with the replica inside the building and on 12 April 1983 with it outside. The calibration factor, in fissions per count of the digital current integrator, was 6.18×10^9 after the 1982 calibration.

The various estimates of power calibration, however, were not in good agreement. A final calibration run was made on 6 August 1984 with three 0.005 inch thick aluminum-wrapped uranium foils on top of the core and radiochemical determination of ^{99}Mo. This run showed how serious the escape of fission products from the thin foils used in the first two runs was. The escape correction was estimated taking into account the presence of the oxide layers on the surfaces of the foils. The correction amounted to a revision upward of approximately 10 % in the reactor fission rate and a revision downward in the fluence per fission. The correction improved the agreement between the fission foil measurements and the independent Feynman variance-to-mean measurements.

Forehand and Hansen[9] made a new S_n calculation of the ratio of fission rates on a radial traverse across the top of the fissile core, where the foils were located, to the core average fission rate. They used more detailed modeling of the reactor interior and obtained 0.831 as the ratio of the fission densitiy on the axis of the core top to the average density. The value used in the original power calibration was 0.913. This change revised the reactor fission level upward approximately another 10 %.

A comparison of the records of the power levels recorded at different times by the ionization chamber on the replica stand to those of other (older) chambers in the building indicated that the new chamber was losing sensitivity at the rate of 4.8 % per year.

A least-squares analysis was made of the radiochemical data (corrected for fission product escape) and the ionization chamber readings (corrected for the drift just mentioned). The results are the revised calibration coefficients shown in Table 3. In addition to the calibration changes shown in the table, small changes were made for different range settings and for changes as faulty resistors were replaced. Complete calibration data for each of the approximately 500 runs of the replica are available.[9] An overall uncertainty of $\pm$ 4 % in these revised calibration factors is estimated. Table 4 gives the correction factors that have to be

Table 3. Reactor Power Calibration Coefficients.

Date	Reactor Location	Calibration Coefficient		Correction Factor
		Old[a]	New[b]	
21 Sep 1982 - 16 Dec 1982	in Kiva II	6.35E−8[c]	5.09E−8	.802
12 Apr 1983 - 31 May 1983	outside	6.18E+9[d]	7.53E+9 exp (0.048t)[e]	f
18 Jul 1983 - 10 Apr 1984	in Kiva II	6.18E+9[d]	7.51E+9 exp (0.048t)[e]	f
7 May 1984 - 13 Aug 1984	outside	6.18E+9[d]	7.53E+9 exp (0.048t)[e]	f

a. Used by experimenters in data reduction examined in this report.
b. Revised power calibration (Forehand and Hansen).[9]
c. "ε_3" value of digital integrator counts per fission (i.e., 6.35×10^{-8}).
d. Fissions per digital current integrator counts on the 10^{-6} range.
e. t in years after 12 Apr 1983.
f. Depends on date of measurement.

Table 4. Reactor Power Correction Factors for Measured Fluences.

Measurement	Dates	Reactor Location	Correction[a] Factor
[12]Robitaille	Sept-Oct 1982	in Kiva II	.802
[14]Griffith	25-29 Apr 1983	outside	.819
[10]Evans 1[b]	3-24 May 1983	outside	.817
[15]Verbinski 1	26 Sep 1983	in Kiva II	.820
[17]Gold 1	16-19 Sep 1983	in Kiva II	1.000[c]
[11]Bennett	21-22 Sep 1983	in Kiva II	.805
[10]Evans 2	26-27 Sep 1983	in Kiva II	.805
[13]Kerr 1	27 Sep 1983	in Kiva II	.824
[13]Kerr 2	13 Mar 1984	in Kiva II	.802
[13]Kerr 3	8 May 1984	outside	.794
[16]Verbinski 2	10 Jul 1984	outside	.789
[17]Gold 2	17-18 Jul 1984	outside	1.000[c]

a. Detailed correction factors supplied by Forehand and Hansen[9] may disagree by a few percent from the general correction factors given.
b. Number identifies different series of measurements.
c. Gold had corrected reactor power levels available for data reduction.

applied to the calibration factors appearing in the published reports of specific experiments.

Calculations. Two sets of MCNP calculations were made to obtain spectra for each of the positions shown in Figure 7 for comparisons with the experimental measurements. The neutrons from the first set of calculations (by P. Soran) were tallied in energy bins from 0.152 eV to 20 MeV to give the overall neutron spectra and total fluences at the 75 and 200 cm locations. In the second set of calculations (by J. Hendricks), only neutrons with energy greater than 0.5 MeV were tracked to the detector locations to improve the Monte

Carlo statistics in the high-energy part of the spectra. The two sets of calculations were joined at the common 0.5 MeV boundary. The MCNP calculations were made with the standard continuous energy representations (Figure 1) of the ENDF/B cross sections. Other calculations, aimed at testing cross-section values and formats and other computer codes, are discussed under "Comparisons with other calculations."

Measurements. Most of the neutron dose to a person is produced by high-energy neutrons. The measurements that give information about the high-energy neutrons are those made with NE-213 scintillators, nuclear track emulsions, foil activation, and sulfur activation. The scintillators, emulsions, and foils give information from which the neutron spectrum can be deduced; the sulfur gives a single result that represents an average of the product of the S(n,p) cross section and the neutron energy spectrum.

The total number of neutrons emitted is also important because a major part of the gamma-ray dose is produced by gamma rays that were produced by neutrons in the air, soil, etc. Measurements that cover most of the energy spectrum are those made with ^{3}He ionization chambers (Evans et al[10]) and proton recoil counters (Bennett and Yule[11]). Measurements that do cover the entire neutron energy spectrum are those made by foil activation and with multisphere moderated neutron detectors.

The first experiments were done by Robitaille and Hoffarth[12] of the Defense Research Establishment Ottawa (DREO) in September and October 1982. The measurements were made inside Kiva II. Fast neutron spectra (between 0.6 and 10 MeV) were measured using a 2 × 1.75 inch NE-213 organic scintillator at 13 of the locations surrounding the casing as shown in Figure 7. Additional integral information was provided by a cadmium-covered boron-trifluoride (BF_3) counter of 1-inch diameter and 8-inch sensitive length, enriched in the concentration of ^{10}B, mounted on the same holder as the NE-213 detector.

With 200 cm between the detector and the center of the core, estimation of the contribution of background neutrons (i.e., those interacting with the detectors after scattering off the walls and floor of the containment building) was accomplished by interposing (with an overhead hoist) a 36 × 36 × 18 inch (91.44 × 91.44 × 45.72 cm) concrete block between the source and the detector. The 18-inch (45.72 cm) thickness of concrete reduced the transmitted fast-neutron fluence by a factor of approximately one hundred, thus rendering the detectors sensitive primarily to room-scattered radiation. At 200 cm, the NE-213 detector was influenced by an observed background contribution of 14 % of the total counting rate for neutron energies above 0.6 MeV at the 90° measurement location. The background contribution to the BF_3 detector at this location was about 65 %. Similar background corrections were obtained at all the other 200 cm locations with the exception of the position at 0° where safety considerations prohibited location of the concrete block directly above the reactor. At 0° the background contribution was expected to be much lower than anywhere else as the reactor itself shielded the detector from the floor beneath, from which a large portion of the scattered neutrons were suspected to originate.

At the 75 cm radius, measurements with the shadow bar were impossible due to the size of the concrete block and the close proximity of the detectors to the assembly. However, at this closer distance, the average neutron count rate seen by the NE-213 detector was approximately 6.5 times larger than the count rate at 200 cm. Since the background counting

rate alone is expected to be relatively invariant to such a change in distance (most scattered neutrons originating from the walls and floor), the average background contribution at 75 cm was estimated to be no more than 2 % of the observed counting rate. No background correction to the NE-213 measurements at 75 cm was therefore made. Similarly the background contribution of the BF_3 measurements at 75 cm was estimated to be approximately 20 % of the observed counting rate. Because of this high background, no results of the BF_3 measurements are discussed. Attempting to use the concrete block as a shadow shield for floor scattered radiation would only serve to introduce another scattering source closer to the detectors than the floor and make the backgrounds worse.

Three sets of sulfur activation measurements were made by Kerr et al[13] of Oak Ridge National Laboratory (ORNL) on 27 September 1983, 13 March 1984, and 8 May 1984. The measurements were made by exposing high purity sulfur pellets 0.95 cm thick by 3.8 cm diameter (density 2.0 g cm^{-3}). The 27 September 1983 measurements were made with the assembly inside Kiva II. Only a few useful results were obtained from this set of measurements. The 13 March 1984 measurements with the assembly inside Kiva II produced a full set of data at various angles and distances from the core of the device. The 8 May 1984 measurements were made with the assembly outside of the kiva and consisted of measurements only in the waist (90°) direction.

A set of spectral measurements was made by Griffith et al[14] of Lawrence Livermore National Laboratory (LLNL) during the week of 25 April 1983 with the assembly outside of Kiva II. They obtained fast neutron spectra using a 5.08 cm diameter by 5.08 cm high NE-213 organic scintillator. Fast-neutron spectra were obtained at 0, 45, and 90° at 200 cm. Low-energy neutron data were obtained by a multisphere system that included a 12.7 × 12.7 mm ^{6}LiI crystal with polyethylene spheres 7.6, 12.7, 20.3, 25.4, and 30.5 cm in diameter. The 7.6 and 12.7 cm spheres were covered with cadmium shells 0.050 inches thick to suppress thermal neutron response. Low-energy data were obtained at 0 and 90° at 200 cm. Background corrections were not made. Assuming that most of the background is from neutron scattering from the ground, the background level for neutron energies above 0.6 MeV can be estimated as approximately 5 % of the observed rate from Robitaille's measurements (14 %) inside the kiva and the square of the ratio of the height of the core center above the ground when inside (2.3 m) and outside (4 m) the kiva. Applying the same arithmetic to the total neutron background leads to an estimate of 65 % $(2.3/4)^2$ or 20 % background contribution to the measured total neutron fluence.

Neutron threshold foil measurements were made by Verbinski and Cassapakis[15] of Science Applications International Corporation (SAIC) on 26 September 1983. The measurements were made with the assembly inside Kiva II. Another set of measurements was made on 10 July 1984 with the assembly outside the kiva.[16] The second measurements were made with four times the number of reactor fissions as in the first measurement and thus had better foil counting statistics. Comparisons were made with the results from this later measurement. The measurements were made by exposing foils of material to the neutrons and counting the activation produced. The foils were exposed bare, in cadmium, or in a 1-inch outer radius ^{10}B sphere. Two measurements were made. The waist (90°) measurement was made with the foils tight against the Little Boy assembly at 14 inches (35.56 cm) from the core center, except for those in the ^{10}B ball which were at 15 inches (38.1 cm). All data were corrected

by Verbinski to 38.1 cm where a calculation of fluence was made by Hendricks.

Background corrections were not made to this data. However, the calculated fluence at the 90°, 38.1 cm location is about 40 times the calculated fluence at the 90°, 200 cm location where background was measured by Robitaille et al.[12] Thus background should be small at the waist. The assembly itself shields the detector on the nose from neutrons scattered from the ground.

Nuclear research emulsions were used by Gold et al[17] of the Hanford Engineering Development Laboratory (HEDL) to characterize the neutron spectra in the energy range 0.37 to 8 MeV. Emulsions were exposed in September 1983 with the replica reactor located in Kiva II and in July 1984 with the assembly outside. The nuclear research emulsions were 200 and 400 μm thick Ilford L-4 films mounted on glass backing. These emulsions, approximately 1 inch by 1 inch, were exposed end-on with the leading edge facing the replica. The emulsions were enclosed inside 0.02 inch thick cadmium buckets to reduce background proton tracks from n,p reactions in impurity nitrogen in the emulsion. After irradiation, the Ilford L-4 emulsions were developed and proton-recoil track lengths measured on the Emulsion Scanning Processor system at HEDL. The proton-recoil track length distribution was transformed into a neutron energy spectrum. Results from the 400 μm emulsions exposed at 90° and 184 cm inside Kiva II in September 1983, and at 0° and 189 cm outside the kiva in July 1984 were reported.

Separate background runs were made with emulsions at about 200 cm and exposed behind polyethylene shadow shields, 12 inches long with 11.8° half angle. Separate plots of foreground and background proton-recoil energy spectra are shown in the report. From other data in the report, the background effect can be established. At the 90°, 184 cm inside location, 465 background tracks with a length greater than 14 μm from an exposure to 6.63 $\times 10^{15}$ reactor fissions were counted, and 4181 tracks were counted from total exposure to 1.83 $\times 10^{15}$ fissions. Thus, the background level in the kiva for neutrons of energy greater than 0.37 MeV was estimated to be only about 3 % at the 90°, 184 cm location. Comparable values at the 0°, 189 cm, outside location are 1127 background tracks for 1.27 $\times 10^{16}$ reactor fissions and 3130 foreground tracks from a total exposure to 8.83 $\times 10^{15}$ reactor fissions. Thus, the background level outside the kiva for neutrons of energy greater than 0.37 MeV was approximately 25 % at the 0°, 189 cm location.

Comparison of Calculations with Measurements. The comparison of calculated and measured quantities from the Little Boy reactor experiments provides information with which to judge the validity of the transport codes and cross sections used in the calculation of the source terms of the Hiroshima bomb.

The calculated and measured quantities that will be compared here are the fluences of neutrons with energies above a minimum, E_{min}, and the (initial) ^{32}P activity induced in sulfur. There is a maximum to the energies considered too, but it is of importance only for the sulfur activation. To treat all of the experimental data the same way, the measured spectra were extrapolated to 20 MeV using an E^{-n} fit to the spectra between 1 and 3.5 MeV. This extrapolation is illustrated in Figures 9 to 11. The figures show that reported values were greater than 10^{-10} MeV^{-1} cm^{-2} per fission neutron. The fact that the experimenters had trouble measuring lower values does not mean that the high-energy neutrons were not there; it

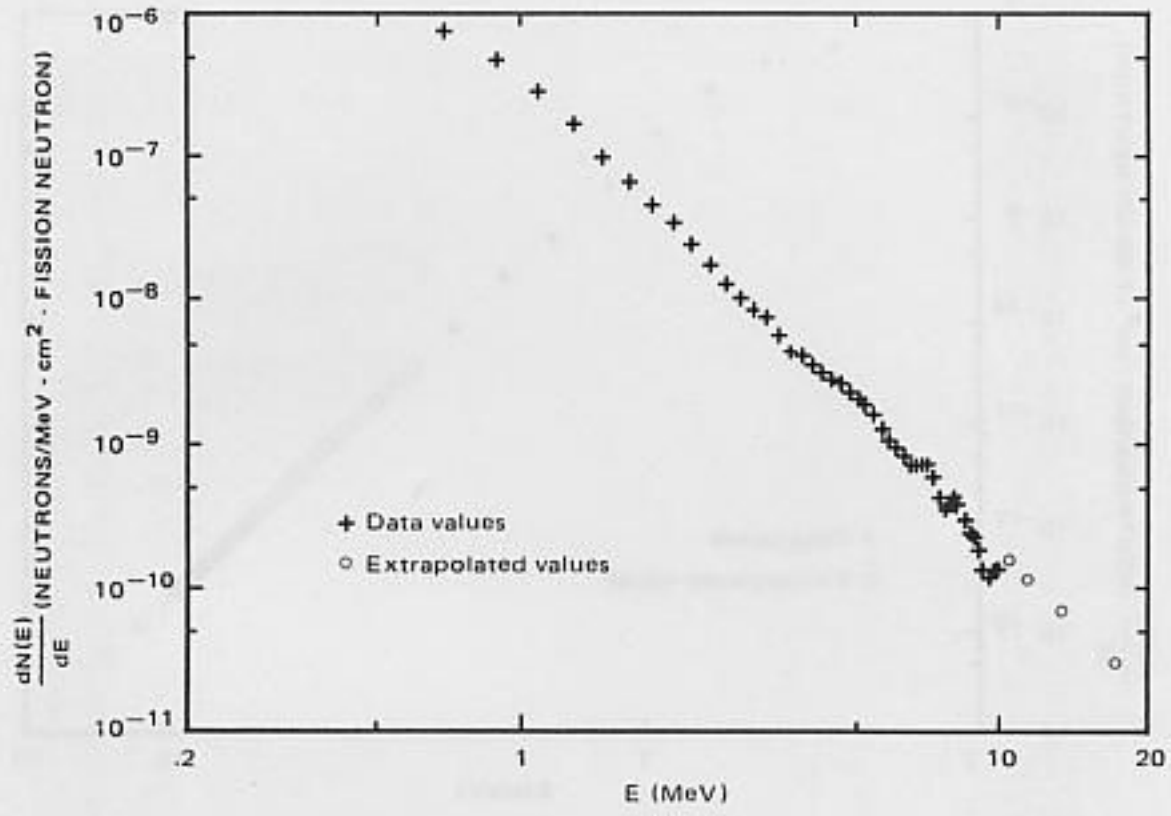

Figure 9. Neutron spectrum measured by Robitaille and Hoffarth[12] at 75 cm and 90° and its extrapolation to 20 MeV.

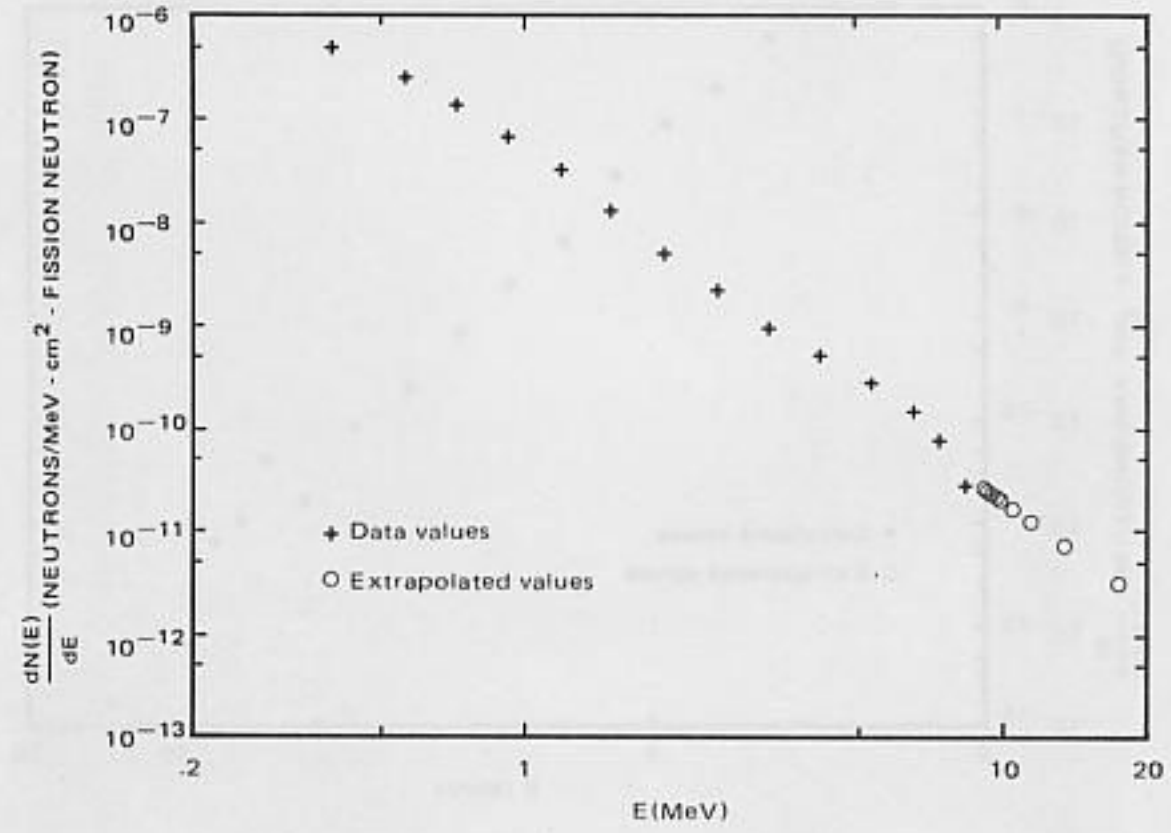

Figure 10. Neutron spectrum measured by Gold et al[17] at 200 cm and 90° and its extrapolation to 20 MeV.

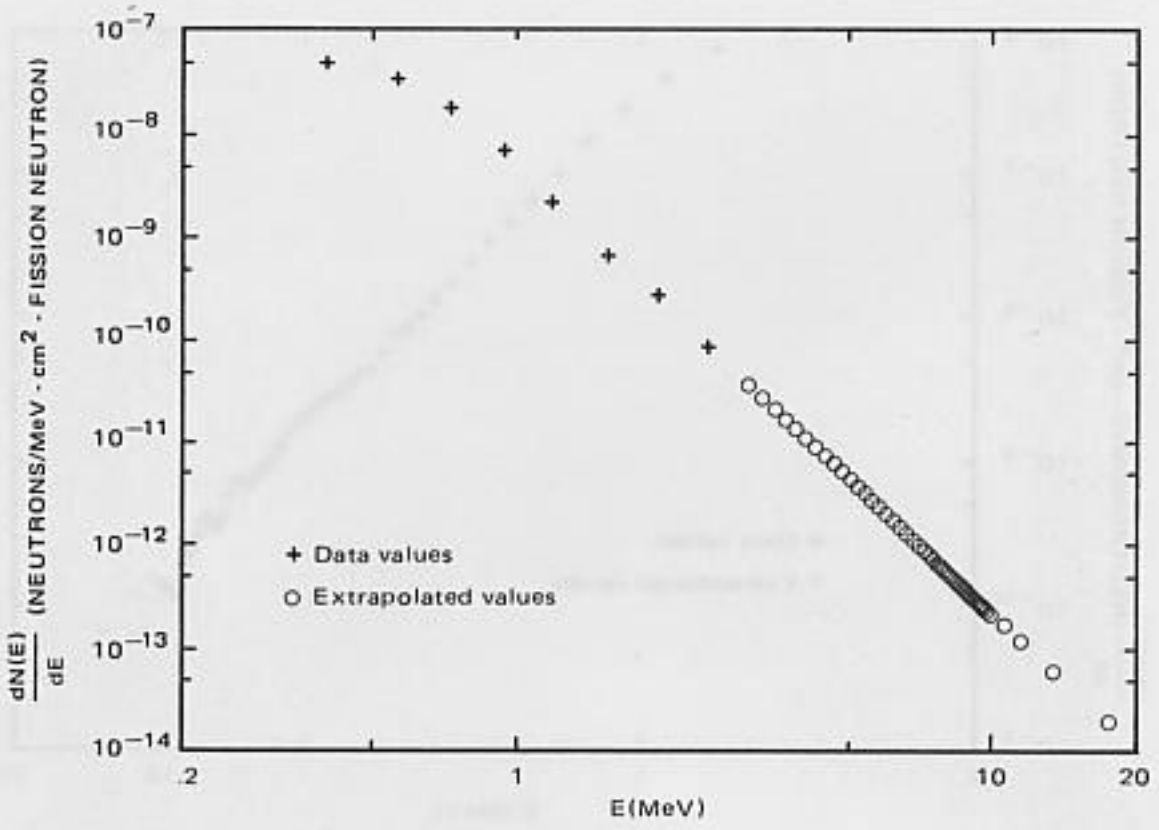

Figure 11. Neutron spectrum measured by Gold et al[17] at 200 cm and 0° and its extrapolation to 20 MeV.

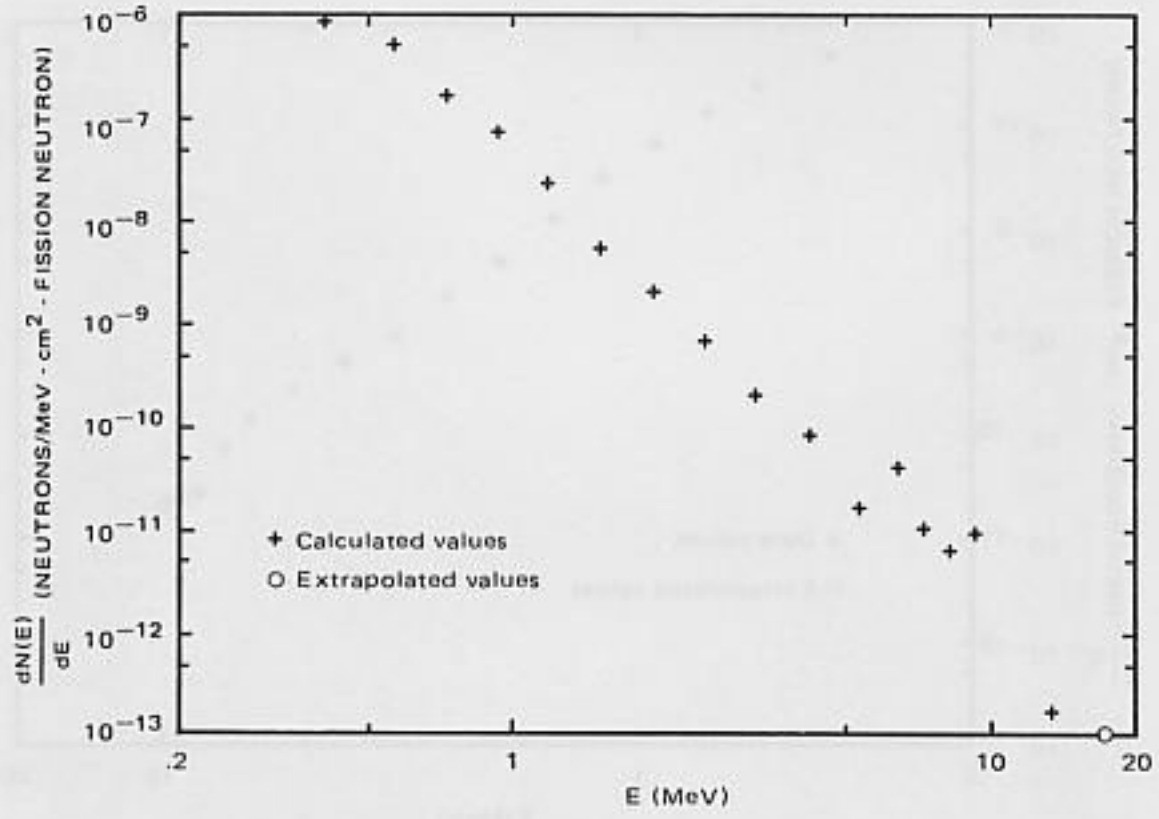

Figure 12. Neutron spectrum calculated by Hendricks at 75 cm and 0° and its extrapolation to 20 MeV.

Table 5. Summary of Measurements Made at the Hiroshima Bomb Replica (Little Boy Reactor).

Angular Direction	Fluence (neutrons/cm²-fission neutron)					^{32}P activity (disintegrations/ minute-g sulfur-fission)	
	E_{min} of integral (MeV)				E_{max} fluence extrapolation to 20 MeV	Extrapolated spectrum	Raw spectrum
	0.0	0.01	0.6	1.0			
Verbinski[15] at 38.1 cm Surface							
90.	2.5080E−05	2.2690E−05	2.4030E−06	8.9610E−07	1.6170E−09	4.2110E−14	4.2120E−14
Verbinski[15] at 66 cm Surface							
0.	2.5170E−06	2.1310E−06	1.0980E−07	2.2390E−08	6.4080E−13	3.4640E−16	3.4650E−16
Robitaille[12] at 75 cm No background correction							
0.			8.1320E−08	1.9770E−08	1.2670E−11	4.5390E−16	4.4860E−16
22.5			6.6560E−08	1.6130E−08	5.4590E−12	3.2550E−16	3.2310E−16
45.0			1.5450E−07	5.0860E−08	1.0800E−10	1.6170E−15	1.5750E−15
67.5			3.1770E−07	1.1810E−07	4.4580E−10	4.6630E−15	4.4990E−15
90.			4.1750E−07	1.6540E−07	8.2540E−10	7.2010E−15	6.9060E−15
112.5			3.5220E−07	1.3210E−07	4.9020E−10	5.1100E−15	4.9290E−15
135.			2.5170E−07	8.5060E−08	1.8490E−10	2.8410E−15	2.7690E−15
Evans[10] at 75 cm Background correction							
90.		4.3930E−06	6.7490E−07	1.9080E−07	1.7800E−08		
Bennett[11] at 75 cm Background correction							
90.		4.3060E−06	5.4730E−07	1.4890E−07	5.3310E−09		
Robitaille[12] at 200 cm Background correction except at 0 degrees							
0.			1.2970E−08	4.4030E−09	2.0460E−11	2.6460E−16	2.5720E−16
45.			2.7690E−08	9.4440E−09	2.3070E−11	3.4260E−16	3.3380E−16
67.5			4.8070E−08	1.7340E−08	6.3580E−11	6.8950E−16	6.6600E−16
90.			5.7640E−08	2.1650E−08	9.5760E−11	9.2430E−16	8.8950E−16
112.5			5.4070E−08	1.9470E−08	7.3810E−11	7.9490E−16	7.6770E−16
135.			4.1810E−08	1.4090E−08	4.2780E−11	5.1790E−16	5.0180E−16
Griffith[14] at 200 cm No background correction							
0.	1.8030E−07	1.5520E−07	1.4360E−08	1.8060E−09	1.8990E−11	2.9890E−17	2.1150E−17
45.			4.5010E−08	8.0870E−09	6.7120E−11	2.6890E−16	2.3440E−16
90.	6.5030E−07	5.9510E−07	8.3630E−08	2.0240E−08	1.4020E−10	9.1350E−16	8.4909E−16
Gold[17] at 200 cm Background correction							
0.			7.1570E−09	1.4440E−09	3.8600E−11	2.3720E−17	9.6430E−18
90.			6.5250E−08	2.1490E−08	1.0970E−10	9.6380E−16	9.1770E−16

merely means that the measurements were difficult. Figure 12 shows a similar extrapolation made to a calculated spectrum; it shows that the extrapolation is consistent with the calculated spectrum within the statistical uncertainties of the Monte Carlo calculation.

Tables 5 to 8 give calculated ^{32}P activities that were produced both with and without the extrapolation. The two procedures result in differences of only a few percent in the 90° direction, where the fluences were high; however, in the 0° direction, where the fluences were low, the differences are sizeable fractions of the activation. Integrals of the measured* neutron spectra, both not-extrapolated and extrapolated to 20 MeV, are given in Table 5 for

*The published data were first corrected by the factors in the last column of Table 4.

Table 6. $^{32}S(n,p)\ ^{32}P$ Cross Sections.

	E(MeV)	σ(barns)		E(MeV)	σ(barns)
1	1.6000E+00	0.0000E+00	42	4.0000E+00	3.0000E−01
2	1.6500E+00	5.0000E−04	43	4.0500E+00	2.9694E−01
3	1.7000E+00	1.0000E−03	44	4.1000E+00	2.9388E−01
4	1.7800E+00	4.6000E−03	45	4.2000E+00	2.8777E−01
5	1.8100E+00	5.9500E−03	46	4.2800E+00	2.8288E−01
6	1.9000E+00	1.0000E−02	47	4.4200E+00	2.7431E−01
7	1.9200E+00	1.1670E−02	48	4.5200E+00	2.6820E−01
8	1.9500E+00	1.4169E−02	49	4.6700E+00	2.5904E−01
9	2.0200E+00	2.0000E−02	50	4.9000E+00	2.4500E−01
10	2.1800E+00	3.6000E−02	51	5.0000E+00	2.4500E−01
11	2.2000E+00	3.8000E−02	52	5.1660E+00	2.4500E−01
12	2.3100E+00	4.9000E−02	53	5.2000E+00	2.4500E−01
13	2.3200E+00	5.0000E−02	54	5.2700E+00	2.4500E−01
14	2.4000E+00	5.8000E−02	55	5.5000E+00	2.6863E−01
15	2.4500E+00	6.3000E−02	56	5.7500E+00	2.9431E−01
16	2.5000E+00	6.8000E−02	57	6.0000E+00	3.2000E−01
17	2.5500E+00	7.3000E−02	58	6.4000E+00	3.2800E−01
18	2.6000E+00	7.8000E−02	59	6.7000E+00	3.3400E−01
19	2.7000E+00	8.8000E−02	60	7.0000E+00	3.4000E−01
20	2.7500E+00	9.3000E−02	61	7.6000E+00	3.5200E−01
21	2.8000E+00	9.8000E−02	62	8.0000E+00	3.6000E−01
22	2.8500E+00	1.0300E−01	63	9.1400E+00	3.6950E−01
23	2.9000E+00	1.0800E−01	64	9.5000E+00	3.7250E−01
24	2.9500E+00	1.1300E−01	65	1.0000E+01	3.7667E−01
25	3.0000E+00	1.1800E−01	66	1.1000E+01	3.8500E−01
26	3.0200E+00	1.2000E−01	67	1.2500E+01	3.1836E−01
27	3.0700E+00	1.2918E−01	68	1.3000E+01	2.9614E−01
28	3.0750E+00	1.3010E−01	69	1.3070E+01	2.9304E−01
29	3.1200E+00	1.3840E−01	70	1.3100E+01	2.9170E−01
30	3.2000E+00	1.5307E−01	71	1.4000E+01	2.5168E−01
31	3.2500E+00	1.6223E−01	72	1.4100E+01	2.4723E−01
32	3.3000E+00	1.7140E−01	73	1.4600E+01	2.2500E−01
33	3.4500E+00	1.9900E−01	74	1.5564E+01	1.7680E−01
34	3.5300E+01	2.1369E−01	75	1.5920E+01	1.5900E−01
35	3.6000E+00	2.2655E−01	76	1.6350E+01	1.3750E−01
36	3.7500E+00	2.5410E−01	77	1.6500E+01	1.3000E−01
37	3.8400E+00	2.7060E−01	78	1.6910E+01	1.2473E−01
38	3.8800E+00	2.7795E−01	79	1.7000E+01	1.2357E−01
39	3.9000E+00	2.8163E−01	80	1.7700E+01	1.1457E−01
40	3.9200E+00	2.8530E−01	81	2.0000E+01	8.5000E−02
41	3.9500E+00	2.9080E−01			

E_{min} of 0, 0.01, 0.6, and 1 MeV and ^{32}P activities are given after folding with the $^{32}S(n,p)\ ^{32}P$ cross section (in Table 6, threshold at 1.6 MeV). The same quantities for calculated spectra are given in Table 7. Table 8 gives the data for measurements of ^{32}P activity in sulfur.

The ratios of calculated to measured quantities versus E_{min} for the directions 90° (waist), 45°, and 0° (nose) are shown in Figures 13 to 15. For these figures, the ^{32}P activity is arbitrarily plotted at 2 MeV. These figures show the effect of the amount of material the neutrons pass through in emerging from the bomb and the effect of the background contamination by neutrons scattered from the surroundings. Figure 13 shows all the data; Figure 14 shows just the data obtained on the surface of the replica (where the contribution of

Table 7. Summary of Calculations Made for the Hiroshima Bomb Replica (Little Boy Reactor)

Angular Direction	Fluence (neutrons/cm²-fission neutron)					^{32}P activity (disintegrations/minute-g sulfur-fission)	
	E_{min} of integral (MeV)				E_{max} fluence extrapolation to 20 MeV	Extrapolated spectrum	Raw spectrum
	0.0	0.01	0.6	1.0			
Hendricks at 38.1 cm Surface ENDF/B cross sections							
90.	2.6310E−05	2.4060E−05	2.6750E−06	9.0160E−07	1.2690E−09	3.6500E−14	3.6370E−14
Hendricks at 66 cm Surface ENDF/B cross sections							
0.	2.8490E−06	2.4840E−06	1.0030E−07	1.9090E−08	1.1220E−12	2.7930E−16	2.7920E−16
Hendricks at 75 cm ENDF/B cross sections							
0.	1.8360E−06	1.6130E−06	7.2040E−08	1.3710E−08	8.0480E−13	2.0050E−16	2.0040E−16
22.5	1.4800E−06	1.3330E−06	6.0110E−08	1.2070E−08	4.7470E−14	1.3450E−16	1.3460E−16
45.	2.4270E−06	2.1870E−06	1.5500E−07	3.9990E−08	4.2860E−12	1.0800E−15	1.0800E−15
67.5	4.8930E−06	3.9000E−06	4.0290E−07	1.2930E−07	1.9640E−10	5.5470E−15	5.5290E−15
90.	5.1820E−06	4.6930E−06	5.2240E−07	1.7610E−07	2.4820E−10	7.1270E−15	7.1030E−15
112.5	4.3670E−06	3.9780E−06	4.1750E−07	1.3900E−07	8.6840E−11	6.4510E−15	6.4420E−15
135.	3.4680E−06	3.1680E−06	2.7970E−07	8.5670E−08	4.2550E−11	2.5690E−15	2.5640E−15
Hendricks at 75 cm ENDF/B V MOD4 iron cross sections							
90.	5.2320E−10		5.0460E−07	1.7210E−07	1.3540E−10	8.2750E−15	8.2750E−15
Pace at 75 cm							
0.	2.2310E−06	2.0590E−06	8.7870E−08	1.1560E−08	1.2110E−13	1.8170E−16	1.8180E−16
22.5	1.7560E−06	1.6370E−06	6.9550E−08	9.1000E−09	8.4930E−14	1.3890E−16	1.3900E−16
45.	2.5390E−06	2.3920E−06	1.8200E−07	3.9300E−08	3.3840E−12	1.0000E−15	1.0000E−15
67.5	4.9440E−06	4.6010E−06	4.7990E−07	1.3280E−07	4.0370E−11	4.7680E−15	4.7690E−15
90.	5.7750E−06	5.3700E−06	6.1450E−07	1.8220E−07	8.1390E−11	7.2380E−15	7.2390E−15
Hendricks at 200 cm ENDF/B cross sections							
0.	1.3050E−07	1.1740E−07	5.9840E−09	1.1760E−09	6.2880E−14	2.0400E−17	2.0390E−17
22.5	1.7940E−07	1.6360E−07	9.6730E−09	2.3000E−09	5.5410E−14	4.2700E−17	4.2720E−17
45.	3.6630E−07	3.3320E−07	2.7620E−08	7.6180E−09	5.5140E−12	2.4650E−16	2.4500E−16
67.5	5.4390E−07	4.9460E−07	5.1480E−08	1.6690E−08	3.1510E−11	7.0220E−16	6.9930E−16
90.	6.3520E−07	5.7740E−07	6.3080E−08	2.1510E−08	4.9470E−11	1.0280E−15	1.0240E−15
112.5	5.9950E−07	5.4200E−07	5.5350E−08	1.7720E−08	1.9250E−11	7.4430E−16	7.4250E−16
135.	5.1080E−07	4.6300E−07	4.2060E−08	1.2970E−08	1.2030E−11	4.5180E−16	4.5060E−16
Hendricks at 200 cm ENDF/B V MOD4 iron cross sections							
90.	6.4150E−07		6.0940E−08	2.0570E−08	1.6390E−11	9.7490E−16	9.7490E−15
Pace at 200 cm							
0.	1.5710E−07	1.4680E−07	6.4060E−08	8.9680E−10	1.0730E−14	1.5360E−17	1.5370E−17
22.5	1.9730E−07	1.8540E−07	1.0830E−08	1.9760E−09	8.2010E−14	3.9480E−17	3.9490E−17
45.	3.9040E−07	3.6570E−07	3.2340E−08	7.8580E−09	1.1920E−12	2.2650E−16	2.2650E−16
67.5	6.0620E−07	5.6650E−07	6.0290E−08	1.6940E−08	5.6160E−12	6.2650E−16	6.2660E−16
90.	6.8870E−07	6.4300E−07	7.2790E−08	2.1560E−08	9.6390E−12	8.7020E−16	8.7040E−16
Pace at surface							
0.	5.1280E−06	4.7330E−06	1.9500E−07	2.3920E−08	1.7870E−13	3.2890E−16	3.2890E−16
22.5	3.5360E−06	3.2790E−06	1.3590E−07	1.6940E−08	1.3880E−13	2.4270E−16	2.4280E−16
45.	6.6050E−06	6.3340E−06	3.5910E−07	5.9140E−08	1.3400E−12	1.1110E−15	1.1110E−15
67.5	2.2190E−05	2.1280E−05	2.1630E−06	5.6680E−07	1.0520E−10	1.7270E−14	1.7270E−14
90.	3.2050E−05	3.0850E−05	3.6510E−06	1.0550E−06	3.0980E−10	3.5130E−14	3.5130E−14

Table 8. Sulfur Activation from ORNL Measurements[13] at the Hiroshima Bomb Replica (Little Boy Reactor)

Sulfur pellet number	Detector distance and direction	Initial ^{32}P activity	
		dpm/g of S per 10^{16} fissions	RSD[a]
27 September 1983[b]			
1-6	Surface - 90°	489	11.2%
1-7	90	479	11.3
1-8	90	471	11.2
1-15	200 cm - 90	12.2	19.4
13 March 1984[c]			
2-1	75 cm - 90	75.1	4.8
2-2	75	62.6	7.3
2-3	67.5	54.0	3.5
2-4	60	35.3	3.7
2-5	45	11.9	4.8
2-6	30	2.01	8.5
2-7	22.5	1.88	10.3
2-8	15	2.14	10.5
2-9	0	2.29	9.7
2-10	Surface - 90	433	3.3
2-11	67.5	89.8	3.4
2-12	45	5.75	3.6
2-13	22.5	3.34	4.5
2-14	0	4.68	8.2
8 May 1984[d]			
3-1	200 cm - 90	9.85	3.41
3-2	90	10.4	3.48
3-3	90	10.2	3.49
3-4	75 cm - 90	82.4	3.37
3-5	90	81.4	3.35
3-6	90	80.7	3.37
3-7	Surface - 90	470	3.39
3-8	90	467	3.39
3-9	90	471	3.39

a. Relative standard deviation of the measured values.
b. Two maximum-power operations inside Kiva II.
c. Three maximum-power operations inside Kiva II.
d. Three maximum-power operations outside Kiva II.

scattered neutrons would be the least) or data were obtained with provisions made to correct for scattering background; and Figure 15 shows the nonsurface data that were obtained with no provision made to correct for scattering background.

As shown in Figure 13, there is a rather wide spread (±15 to 25%) in the measured data in the 90 and 45° directions and a larger spread (±20 to 40%) in the measured data in the 0° direction when all of the measurements are included. The measurements appear to be more consistent with each other in the 45 and 0° directions and no worse in the 90° direction when only the subset of measurements made at the surface of the Little Boy reactor or the subset with corrections for background is considered as shown in Figure 14. The set of measurements made with no background corrections is shown in Figure 15. The difference

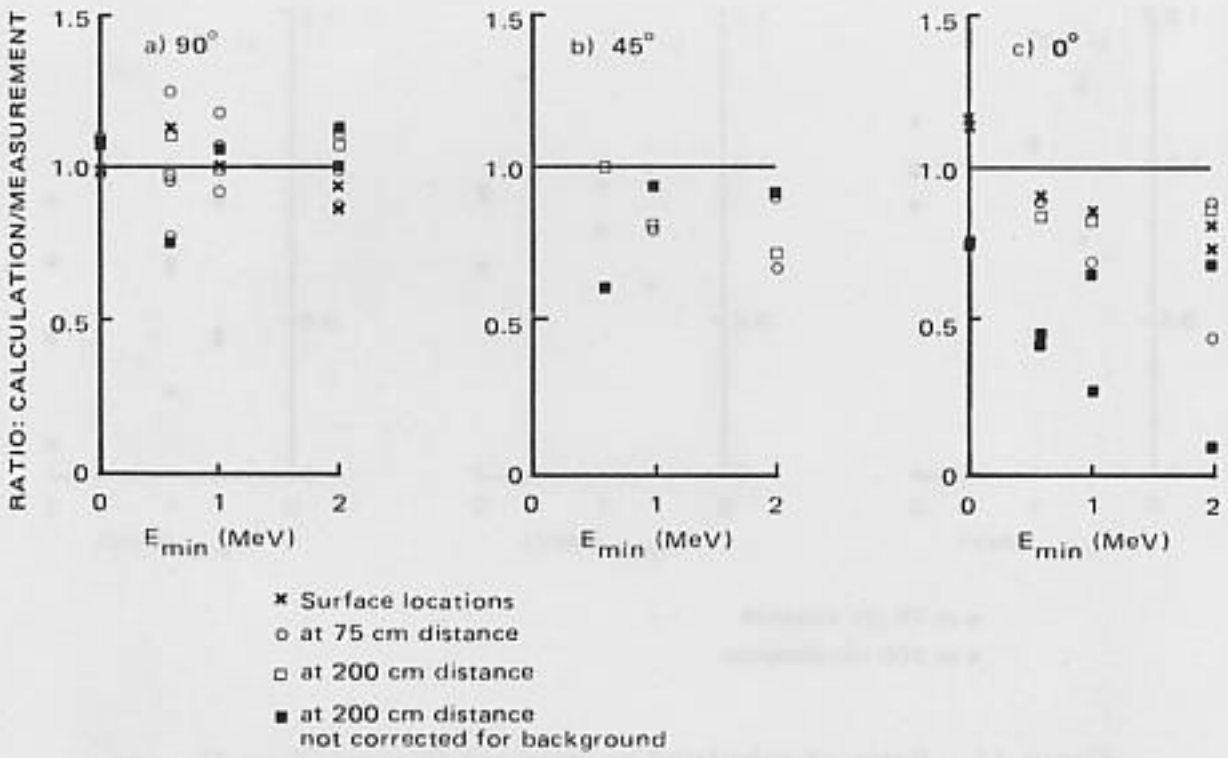

Figure 13. Ratio of calculated to measured fluences (from E_{min} to 20 MeV) and ^{32}P activity (plotted at 2 MeV) for all measurements.

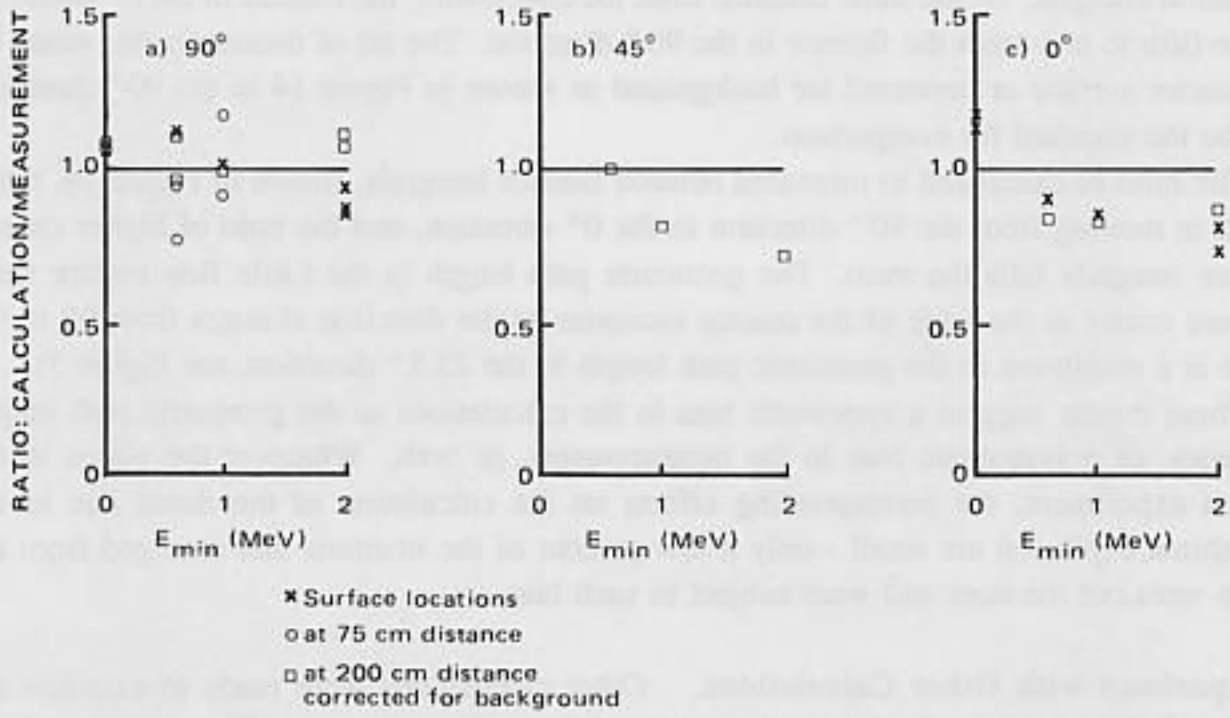

Figure 14. Ratio of calculated to measured fluences (from E_{min} to 20 MeV) and ^{32}P activity (plotted at 2 MeV) for measurements on the surface or with background correction.

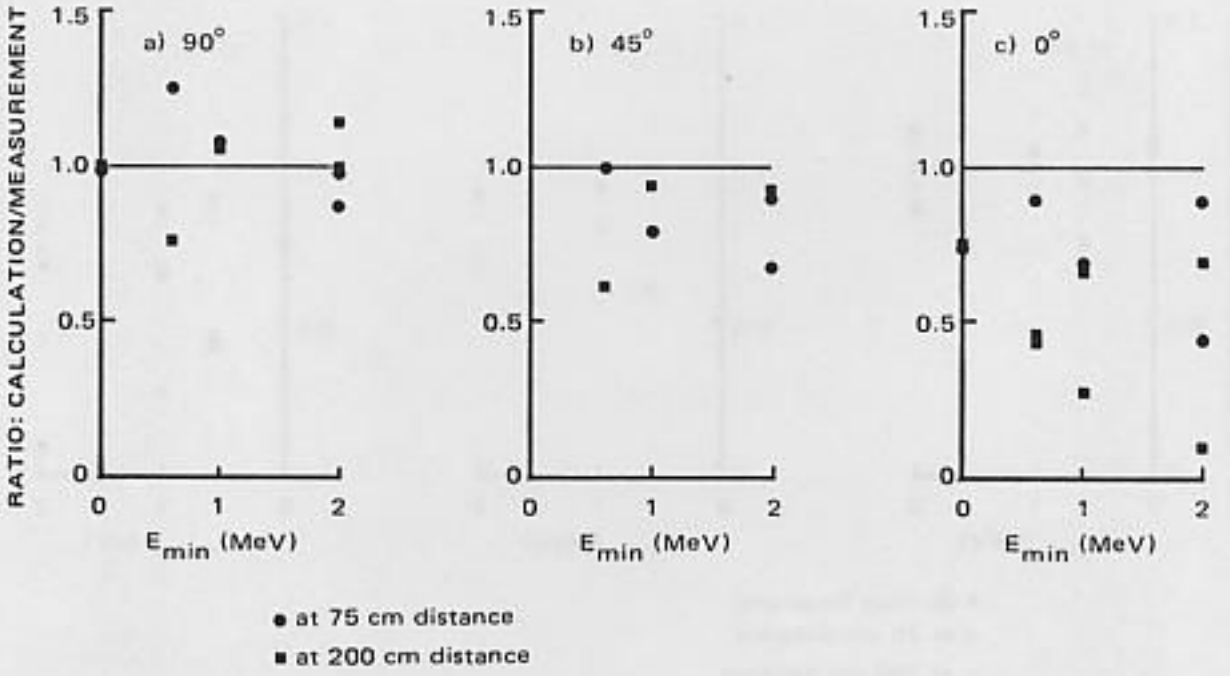

Figure 15. Ratio of calculated to measured fluences (from E_{min} to 20 MeV) and ^{32}P activity (plotted at 2 MeV) for nonsurface measurements without background correction.

between these measurements made without background corrections accounts for most of the spread appearing in Figure 13. Evidently, background effects dominate the measurements made at the 75 or 200 cm distances in the 0° direction at all energies, including the sulfur activation energies. At the same distance from the core center, the fluence in the 0° direction is one-fifth to one-tenth the fluence in the 90° direction. The set of measurements made on the reactor surface or corrected for background as shown in Figure 14 in the 90° direction will be the standard for comparison.

The ratio of calculated to measured neutron fluence integrals, shown in Figure 14, tends to fall in moving from the 90° direction to the 0° direction, and the ratio of higher energy fluence integrals falls the most. The geometric path length in the Little Boy reactor from the core center to the edge of the reactor increases as the direction changes from 90 to 0° (there is a maximum in the geometric path length in the 22.5° direction, see Figure 7).

These results suggest a systematic bias in the calculations as the geometric path length increases, or a systematic bias in the measurements, or both. Whatever the biases in the replica experiment, the corresponding effects on the calculation of the doses due to the Hiroshima explosion are small - only a few percent of the neutrons that emerged from the bomb went out the nose and were subject to such bias.

Comparisons with Other Calculations. Other calculations were made to examine the effects of changes in the formats or the values of the cross sections and for comparison with other computer codes.

MCNP calculations were made with a finer (128 bin) resolution in the angular scattering. They produced no effect on the calculated leakage spectrum, indicating that the standard

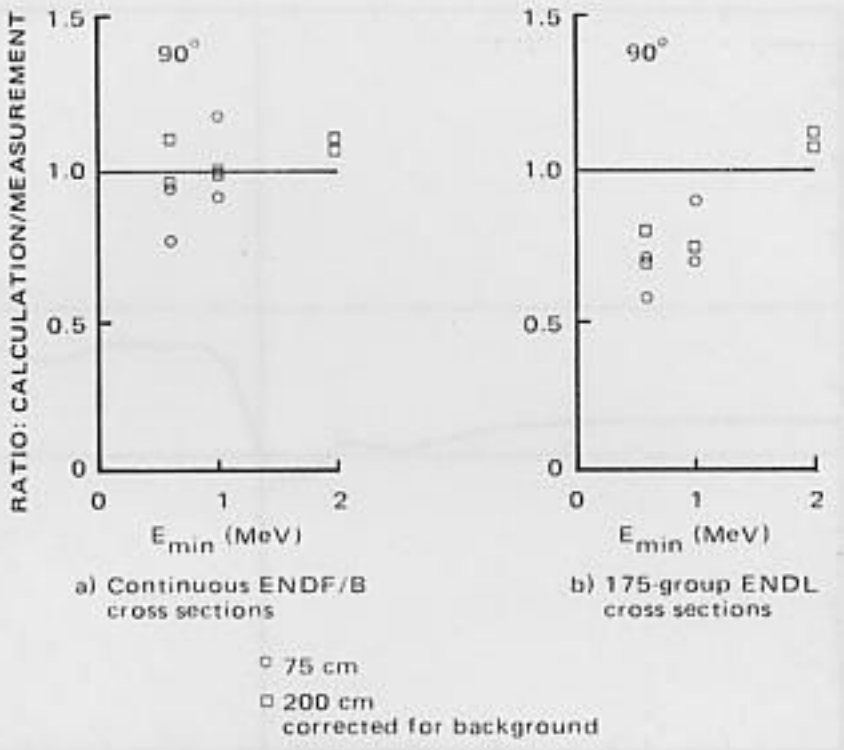

Figure 16. Effect of changing the cross section format on the ratios of calculated to measured fluences (from E_{min} to 20 MeV) and ^{32}P activities (plotted at 2 MeV). Measurement in 90° direction with background correction.

32-bin representation was adequate.

The results of an MCNP calculation for the detectors in the 90° direction using 175-group ENDL representations of the cross sections are shown in Figure 16. Only equivalent data are shown in the two parts of the figure. There is a noticeable deterioration in the agreement between calculation and measurement with group cross sections.

A similar comparison of the effects of discrete and continuous representations of the iron cross sections is shown in Figure 17. The ratio of the integrals of the fluence distribution from an energy, E_{min}, to 20 MeV are shown from calculations of a one-dimensional model of the Hiroshima bomb explosion. The ratio of the results from a 240-group cross-section set to the results from a continuous cross-section set are shown. The same drop in the ratio from 2.0 to 0.6 MeV is seen in this comparison as in Figure 16. The integral above 0.6 MeV, calculated using multigroup cross sections, is about 25 % lower than the same integral using continuous cross sections.

This effect on the neutron leakage spectrum from Monte Carlo calculations, made with grouped cross sections, is due to the difference between the representation of cross sections that have resonances, (e.g., the cross section of iron shown in Figure 1) and becomes important only in deep penetration calculations.

The effect is a spectral shift; the neutrons are in the spectrum but at the wrong energies. The total neutron fluences at the surface of the bomb, the integrals over the differential fluences from 0 to 20 MeV, for the grouped and continuous methods differ by less than the

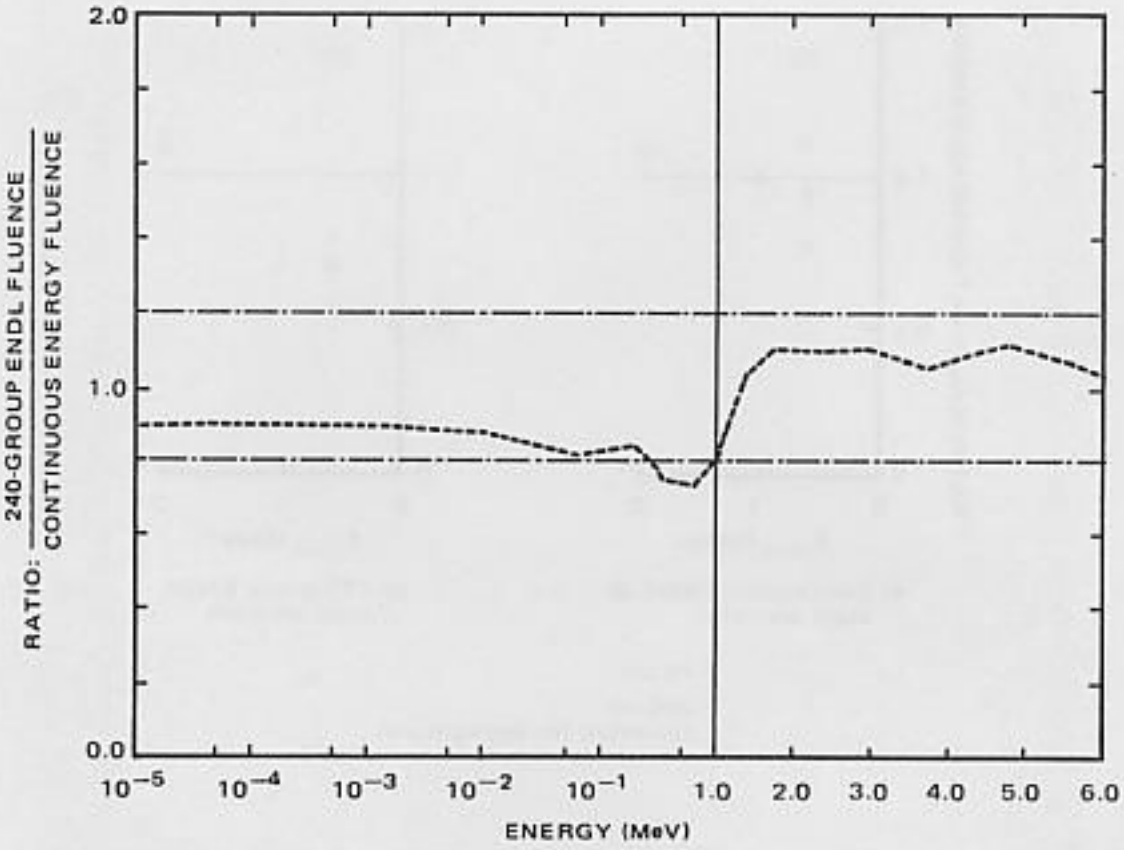

Figure 17. Ratio of the fluence above the energy shown on the abscissa calculated with the 240-group ENDL library and with a continuous library from ENDF/B.

25 % of the integral from 0.6 to 20 MeV. The difference in the total neutron fluence in the transmission of seven mean free paths of nitrogen due to the cross-section representation is given as 9 % by Plechaty.[18] The difference in the total neutron output of the Hiroshima weapon from the one-dimensional calculations using continuous and multigroup ENDF/B cross sections was 10 % (the multigroup output was the lower) and the difference in the fluence of neutrons with energies between 0.6 and 20 MeV was 20 %.

To test a different transport method, Pace at ORNL calculated the Little Boy reactor spectrum at 15 locations, using discrete ordinates (or S_n) techniques and 37-group cross sections from the Vitamin-E ENDF/B-V library. The comparisons of the Pace calculation with measurements are shown in Figure 18. There is an apparent bias for the Pace calculations to be high at low energies and low at high energies.

The results of reactor physics studies of deep penetration problems in iron, using S_n calculations, consistently indicate that the values of the inelastic cross section for iron (ENDF/B Mod-3) are too large in a certain energy range, and/or energy-angle correlation in the inelastically scattered neutrons in the continuum is needed.[19] Combining these considerations with considerations of microscopic data and consistent nuclear model analysis led to the Mod-4 update of the ENDF/B iron cross sections.

The ratio of continuous-energy MCNP calculations, using the Mod-4 iron cross sections, to measurements is shown in Figure 19. The changes made to the Mod-4 iron cross section

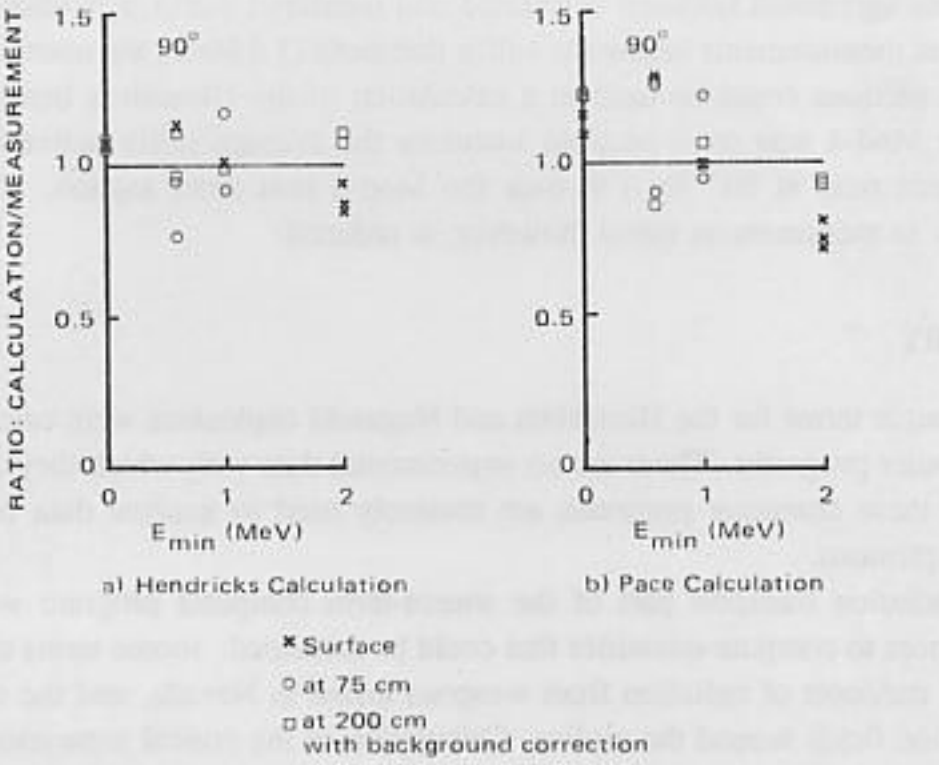

Figure 18. Effect of changing from a Monte Carlo to an S_n transport calculation on the ratio of calculated to measured fluences (from E_{min} to 20 MeV) and ^{32}P activity (plotted at 2 MeV). Measurement in 90° direction with background correction.

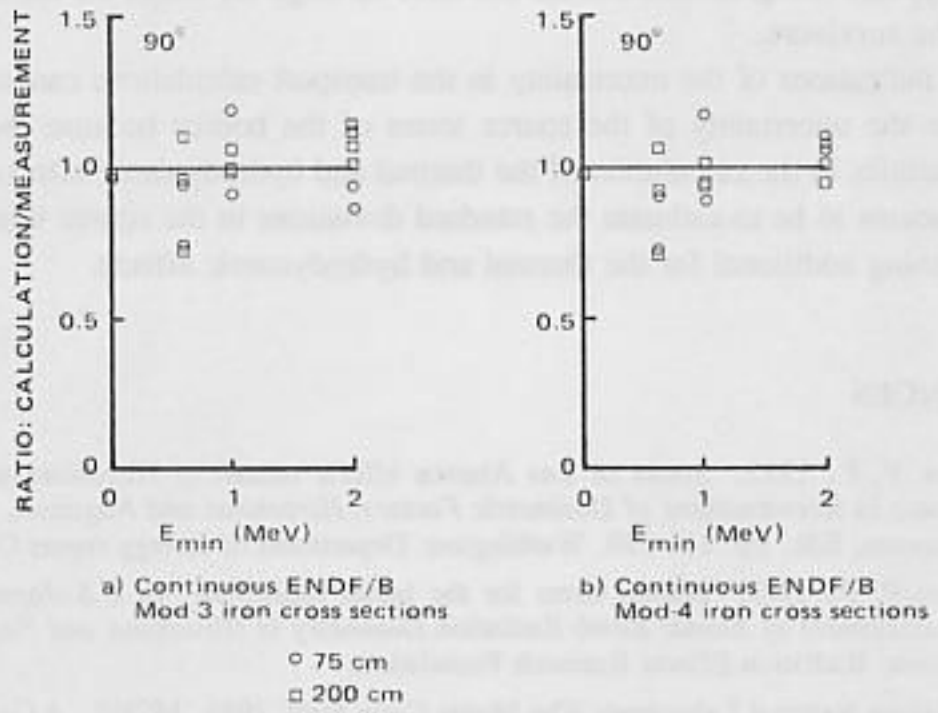

Figure 19. Effect of changing from the Mod-3 cross sections for iron to the Mod-4 on the ratio of calculated to measured fluences (from E_{min} to 20 MeV) and ^{32}P activity (plotted at 2 MeV).

improve the agreement between calculated and measured sulfur activation values. Fluence and spectral measurements below the sulfur threshold (1.6 MeV) are unchanged. The Mod-4 iron cross sections could be used in a calculation of the Hiroshima bomb explosion. The use of the Mod-4 iron cross sections increases the average sulfur activation calculation to measurement ratio at 90° by 1 % over the Mod-3 iron cross section. The spread in the calculation to measurement ratios, however, is reduced.

SUMMARY

The source terms for the Hiroshima and Nagasaki explosions were calculated with complex computer programs. There are no experimental data with which they can be compared. However, these computer programs are routinely used to analyze data from underground nuclear explosions.

The radiation transport part of the source-term computer program was used in other circumstances to compute quantities that could be measured: source terms of reactors, source terms and transport of radiation from weapons tested in Nevada, and the critical separation and radiation fields around the replica. Calculation of the critical separation is an especially sensitive test of total and absorption cross sections, and the calculation for the replica agreed with experiment within the experimental errors. The calculations for the neutron fluence out the waist of the replica, where the amount of material traversed was least, were within a range of ± 25 % of the measured values (Figure 14) where the spread is in the measured values. Although these data do not represent a random selection from a population, their standard deviation of 11 % is noted. The calculations and measurements for other directions show growing disagreement, but no worse than 30 %, as the amount of material increases. Fortunately, this disagreement should not have as large an effect on the calculation of the doses to the survivors.

These indications of the uncertainty in the transport calculations cannot be carried over to estimate the uncertainty of the source terms of the bombs because they do not reflect the uncertainties in the calculation of the thermal and hydrodynamic effects. A conservative approach seems to be to estimate the standard deviations in the source terms as about 20 % plus something additional for the thermal and hydrodynamic effects.

REFERENCES

1. Whalen, P. P., 1982. Status of Los Alamos efforts related to Hiroshima and Nagasaki dose estimates. In *Reevaluations of Dosimetric Factors, Hiroshima and Nagasaki*, V. P. Bond and J. W. Thiessen, Eds., pp. 111-130. Washington: Department of Energy report CONF-810928.
2. Whalen, P. P., 1983. Source terms for the initial radiations. In *U.S.-Japan Joint Workshop for Reassessment of Atomic Bomb Radiation Dosimetry in Hiroshima and Nagasaki*, pp. 13-44. Hiroshima: Radiation Effects Research Foundation.
3. Los Alamos National Laboratory, The Monte Carlo Staff, 1986. *MCNP - A General Monte Carlo Code for Neutron and Photon Transport*, J. F. Briesmeister, Ed. Los Alamos, NM: Los Alamos National Laboratory, manual LA-7396-M, Rev. 2.
4. Magurno, B. A., Kinsey, R. R., and Scheffel, F. M., 1982. *Guidebook for the ENDF/B-V Nuclear Data Files*. Brookhaven, NY: Brookhaven National Laboratory, Electric Power Research Institute

report NP-2510.

5. Preeg, W. E., 1976. Letter to C. P. Knowles. Published as an appendix to Whalen.[1]
6. Auxier, J. A., 1977. *ICHIBAN: Radiation Dosimetry for the Survivors of the Bombings of Hiroshima and Nagasaki.* Washington: Department of Energy, report TID-27080.
7. Thorngate, J. H., Johnson, D. R., and Perdue, P. T., 1966. *Neutron and Gamma-Ray Leakage from the ICHIBAN Critical Assembly.* Washington: Department of Energy, report CEX-64.7.
8. Whalen, P. P., Soran, P. D., Malenfant, R., and Forehand, H. M., Jr., 1983. Experiments at Los Alamos National Laboratory with the replica of the Hiroshima weapon. In *Second U.S.-Japan Joint Workshop for Reassessment of Atomic Bomb Radiation Dosimetry in Hiroshima and Nagasaki,* pp. 21-25. Hiroshima: Radiation Effects Research Foundation.
9. Forehand, H. M. and Hansen, G. E., 1985. *Power Calibrations and Irradiation Histories of the Little Boy Comet Assembly for the Period 9/21/82 - 8/13/84.* Los Alamos, NM: Los Alamos National Laboratory, report Q2-85-WP5.
10. Evans, A. E., Bennett, E. F., and Yule, T. J., 1984. *Little Boy Neutron Spectrum Below 3 MeV.* Los Alamos, NM: Los Alamos National Laboratory, report LA-UR-84-1523.
11. Bennett, E. F. and Yule, T. J., 1984. *Neutron Spectrum Measurements Using Proton Recoil Proportional Counters: Results of Measurements of Leakage Spectra for the Little Boy Assembly.* Argonne, IL: Argonne National Laboratory, report ANL-EV-AP-84-2.
12. Robitaille, H. A. and Hoffarth, B. E., 1983. *Neutron Leakage from COMET - a Duplicate Little Boy Device.* Ottawa: Defense Research Establishment, report 878.
13. Kerr, G. D., Emery, J. F., and Pace, J. V., III, 1985. *Sulfur Activation at the Little Boy-Comet Critical Assembly: A Replica of the Hiroshima Bomb.* Oak Ridge, TN: Oak Ridge National Laboratory, report ORNL/TM-9439.
14. Griffith, R. V., Huntzinger, C. J., and Thorngate, J. H., 1984. *Neutron Spectra as a Function of Angle at Two Meters from the Little Boy Assembly.* Livermore, CA: Lawrence Livermore National Laboratory, report UCRL-90178.
15. Verbinski, V. V. and Cassapakis, C. G., 1984. *Neutron Threshold-Foil Spectral Flux Measurements Compared with LANL Monte Carlo Calculations for Little Boy Replica.* San Diego, CA: Science Applications International Corporation, report SAI-83-1128.
16. Verbinski, V. V., 1985. Personal communication.
17. Gold, R., Roberts, J. H., and Preston, C. C., 1985. *Nuclear Research Emulsion Neutron Spectrometry at the Little-Boy Replica.* Richland, WA: Westinghouse Hanford Company, report HEDL-7559.
18. Plechaty, E. F., 1982. *The Effect of Resonance Structure on 14 MeV Monte Carlo Neutron Transport in Nitrogen and Air.* Livermore, CA: Lawrence Livermore National Laboratory, report UCID-19583.
19. Fu, C. X. and Hetrick, D. M., 1986. *Update of ENDF/B-V Mod-3 Iron: Neutron-Producing Reaction Cross Sections and Energy-Angle Correlations.* Oak Ridge, TN: Oak Ridge National Laboratory, report ORNL/TM-9964.